8-2017

# Multifuntional Nanotherapeutics for the Combinatorial Drug and Gene Therapy in the Treatment of Glioblastoma Multiforme

Breanne Hourigan
*Clemson University*, bhourig@g.clemson.edu

# MULTIFUNTIONAL NANOTHERAPEUTICS FOR THE COMBINATORIAL DRUG AND GENE THERAPY IN THE TREATMENT OF GLIOBLASTOMA MULTIFORME

---

A Thesis
Presented to
the Graduate School of
Clemson University

---

In Partial Fulfillment
of the Requirements for the Degree
Master of Science
Bioengineering

---

by
Breanne Hourigan
August 2017

---

Accepted by:
Jeoung Soo Lee, Ph.D., Committee Chair
Brian Booth, Ph.D.
Michael Lynn, M.D.

ABSTRACT

Glioblastoma multiforme (GBM), a grade IV glioma, is the most common type of primary brain tumor, affecting about 3 out of 100,000 persons per year in the United States. GBM accounts for about 80% of primary malignant brain tumors, and is also the most aggressive of malignant brain tumors. With exhaustive treatment, survival only averages between 12 and 15 months, with a 2-year survival rate less than 25%. New therapeutic strategies are necessary to improve the outcomes of this disease. Chemotherapy with temozolomide (TMZ), a DNA alkylating agent, is used as a first-line of treatment for GBM. However, GBM tumors develop resistance to TMZ over time due to increased expression of $O^6$-methylguanine-DNA methyltransferase (MGMT), a gene responsible for DNA repair.

We previously developed cationic, amphiphilic copolymer poly(lactide-co-glycolide)-g-polyethyleneimine (PgP) and demonstrated its utility for nucleic acid delivery. Here, we examine the ability of PgP polyplexes to overcome TMZ resistance and improve therapeutic efficacy through combination drug and gene therapy for GBM treatment. In this study, we evaluated the ability of PgP to deliver siRNA targeting to MGMT (siMGMT), a gene responsible for drug resistance in GBM. Our results demonstrated that PgP effectively forms stable complexes with siRNA and protects siRNAs from heparin competition assay, serum- and ribonuclease-mediated degradation, confirming the potential of the polyplex for *in vivo* delivery. Results from MTT assays showed that PgP/siRNA polyplexes exhibited minimal cytotoxicity compared to untreated cells when incubated with T98G human GBM cells. We also demonstrated that PgP/siMGMT polyplexes mediate knockdown of MGMT protein as well as a significant ~56% and ~68%

knockdown of MGMT mRNA in T98G GBM cells compared to cells treated with PgP complexed with non-targeting siRNA (siNT) at a 60:1 and 80:1 nitrogen:phosphate (N:P) ratio, respectively.

Further, co-incubation of PgP/siMGMT polyplexes with TMZ enhanced therapeutic efficacy in T98G GBM cells compared to treatment with the polyplex or TMZ alone. After generation of athymic mouse GBM model, PgP/siMGMT polyplexes were locally injected into the tumor. Relative to untreated injury only, PgP/siMGMT polyplexes significantly reduced MGMT mRNA and protein expression at 3 days post-injection. These studies demonstrate that PgP is an efficient non-viral delivery carrier for therapeutic siMGMT to the tumor cells and may be a promising platform for the combinatorial siRNA/drug therapy for GBM treatment. In the future, we will study the therapeutic efficacy of the combination of PgP/siMGMT and TMZ in athymic mouse GBM model.

DEDICATION

I would like to dedicate my work to my parents Maureen and John, and my sisters Phoebe and Chloe. You all inspire me every day with your youthfulness and wisdom, and I thank you for your never-ending support and love.

ACKNOWLEDGEMENTS

I'd like to thank my advisor, Dr. Jeoung Soo Lee, for not only giving me guidance in my research, but also pushing me to be the best person I can be. I would like to thank Angela Alexander-Bryant for being the best mentor and teammate I could have asked for. I'd like to thank Christian Macks for helping me with every odd problem that I encountered, and thank you to the rest of the 4D lab members that have helped me including So Jung Gwak, Erica Beal, and Noah Cecil.

I'm thankful for my committee members Dr. Lynn, Dr. Booth and Dr. Webb, and would like to thank the COBRE grant for funding this research.

TABLE OF CONTENTS

Page

TABLE OF CONTENTS (CONTINUED)

Page

LIST OF FIGURES

Figure

Page

CHAPTER 1

# INTRODUCTION & BACKGROUND

Each year over 25,000 new malignant brain tumors are to be diagnosed in the United States. With 700,000 Americans currently living with malignant brain tumors, over 170,000 are expected to die this year due to the cancer. With a median age of diagnosis of 64, brain tumors may seem to be a factor of aging, but they are also the most common cancer occurring in children under the age of 15. Brain tumors are the leading cause of cancer-related death in children between the ages of 0 and 14, and the third most common cancer-related death in young adults between the ages of 15 and 39.[1]

There are more than 100 distinct types of primary brain and central nervous system tumors, the most common being meningiomas and gliomas. Meningiomas make up 36.6% of all primary brain tumors, but gliomas make up 74.6% of all malignant brain tumors. Gliomas arise from the glial, or supportive cells in the brain, such as astrocytes or oligodendrocytes.[2] Glioblastoma multiforme (GBM) is a high-grade glioma that arises from astrocytes, making it a type of astrocytoma. The World Health Organization (WHO) assigns four grades to astrocytomas, where glioblastomas make up grade IV.[3,4] GBM makes up about 55% of all gliomas, affects about 3 in 100,000 people, and an estimated 12,400 new cases are predicted in 2017. Glioblastomas are

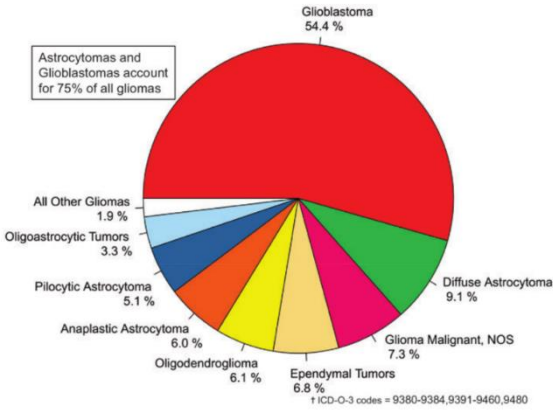


*Figure 1.* The CBTRUS (Central Brain Tumor Registry of the United States) reports distribution of histological subtypes of primary brain and CNS gliomas, where GBM makes up 54.4% (N= 92,504). 1

not only the most common malignant primary brain tumor, but also the most aggressive.[5] Without treatment, the survival rate for GBM is 2-3 months, and with aggressive treatment, survival averages between 12 and 15 months.[6,2] The five year survival rate is less than 5%, due in part to inefficacy of treatment modalities.[4] GBM is about 2 times more common in whites than blacks, and 1.5 times more common in men than in women.[1] Clinically, patients present with headaches, neurological symptoms such as confusion, memory loss, seizures or personality change.

The current standard of care for treating GBM includes maximal surgical resection of the tumor, radiation therapy and chemotherapy via temozolomide (TMZ).[7] Carmustine (BCNU, Gliadel ™) wafers have been used as adjuvant local therapy in combination with systemic TMZ, but use has been limited due to observed toxicities and ambiguity of overall survival benefit.[8,9] Additionally, bevacizumab, a monoclonal antibody for the inhibition of vascular endothelial growth factor (VEGF), has been used since its approval as a treatment for recurrent glioblastomas.[10] However, the 2-year survival rate after treatment remains at about only 25%.[11] GBM remains an essentially incurable disease, with recurrences taking place in most cases. High grade gliomas tend to be not only located in undesirable locations in the cerebral hemispheres, but they also have high rates of invasion into surrounding brain tissue. These factors allow for persistent tumor growth, and low chance of patient remission. Most adult gliomas are classified as diffuse gliomas, where the tumor cells diffuse into normal preexisting brain tissue. Most low grade diffuse gliomas will eventually develop into grade III or grade IV gliomas.[3,11]

### 1.1 Etiology

Primary brain tumors are histologically highly heterogeneous, where even between studies classifications and groupings of tumors often differ. The name glioblastoma "multiforme" is indicative of its heterogeneity. GBM is multiforme grossly, where some regions are necrotic, where others are hemorrhagic. On the microscopic level, regions can be found of pleomorphic nuclei, pseudopalisading necrosis, as well as microvasculature proliferating. GMB is genetically multiforme where various mutations, increased expression, or deletions cause tumorgenicity.[5]

Histologically, glioblastoma can be diagnosed or confirmed in part due to the patterns of necrotic areas that occur within the tumor. The most common or symbolic of which is the pseudopalisading necrosis, where many small irregularly shaped necrotic foci are within dense-packed, radially oriented glioma cells. The necrotic regions are highly hypoxic, and have shown to express high amounts of hypoxia-inducible factor 1a (HIF-1a), and produce increased quantity vascular endothelial growth factor (VEGF), which attempt to allow for inflammation and angiogenesis in the necrotic regions.[12] The next most common necrotic pattern is described as having large regions of necrosis, with necrotic tumor cells and vessels. This type contains an intact layer of glioma cells surrounding a vessel, likely having becoming ischemic with lack of blood supply. This second type of large necrotic areas is found in almost all primary GBM, compared with only half of secondary GBM.[13]

Etiologically, various risk factors have been linked to the onset of GBM, including smoking unfiltered cigarettes, petroleum refining work, and synthetic rubber manufacturing.[14] Other environmental risk factors include exposure to ionizing radiation, such as therapeutic,

exposure to vinyl chloride and to pesticides. A study done by Burch et al. showed that adults with brain tumors reported more use of hair dye and hair spray compared to control.[15] The Central Brain Tumor Registry of the United States (CBTRUS) created the map shown in Figure 2 using data from 2006 to 2010, displaying distribution of malignant primary brain tumors throughout the United States. Geography and environmental factors pertaining to location display possible correlation of malignancies with the northern regions of the United States. [1]

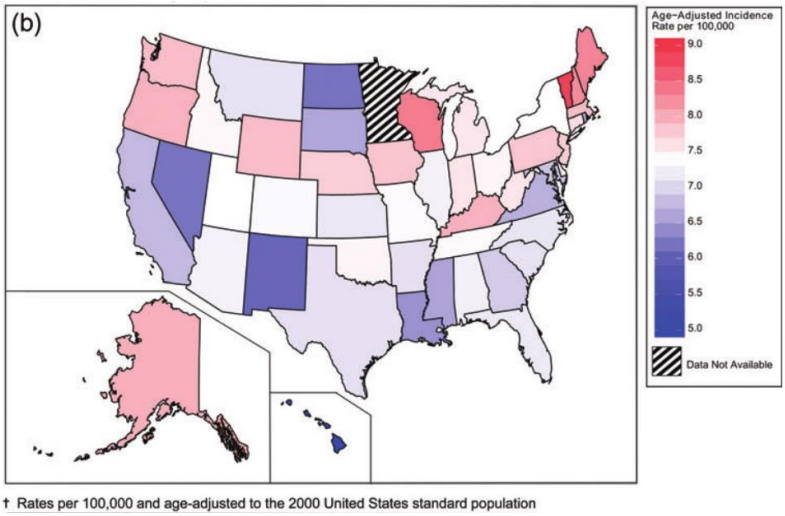


*Figure 2.* The CBTRUS (Central Brain Tumor Registry of the United States) reports distribution of average incidence rates of malignant primary brain and CNS tumors across the US.[1]

Zahm et al. summarized 17 studies done on the relationship between pesticide exposure and pediatric brain tumors. Pesticide exposure was considered a mother using household pesticides or insecticides, a father working in an agricultural setting, and child contact with pets. Nine out of 17 studies showed statistically significance between exposure and brain tumor development, while 5 studies showed nonsignificant correlation, and 3 studies showed no association.[16] Factors including exposure to electromagnetic fields (EMF), formaldehyde, diagnostic radiation, and mobile phones have not be proven to be linked with the onset of GBM.[2] Hereditary syndromes, such as tuberous sclerosis and neurofibromatosis, family history,

and allergies have also been studied as risk factors. [14] Although many factors have been extensively studied, data is inconclusive in providing definitive measures for the prevention or early diagnosis of GBM.

**1.2 Pathogenesis**

Glioma development occurs due to sequential acquisition of genetic alterations, causing a transformation from benign to malignant tissue.[17] Glioblastoma occurs in four clinical subtypes, but most commonly in the form of classical, or primary GBM, and proneural, or secondary GBM[18] . Classical GBM arises *de novo,* and occurs in about 95% of cases, only taking about 3-6 months to develop. Proneural, or secondary GBM arises as a recurrence from a previous anaplastic or low-grade astrocytoma, usually taking 10-15 years to develop.[13,2] Classical GBM can be classified by increased expression of mutated epidermal-growth factor receptor (EGFR), whereas secondary GBM has increased expression of platelet-derived growth factor (PDGF-A) receptor. Various genetic alterations have been identified to lead to malignant transformation and several will be described following.

Classical GBM presents not only with EGFR amplification, but almost always with an amplification of chromosome 7 and a loss of chromosome 10. EGFR amplification is found in the majority of classical cases.[18] It can be found in a mutated form, with a truncation due to deletion of exons 2-7. The mutated EGFR causes activation of the Ras-Sch-Grb2 pathway, allowing for proliferation and suppression of apoptosis, and enhanced tumorgenicity. Commonly, primary GBM presents with a phosphate and tensin homologue (PTEN) mutation and/or a p16INK4a deletion as well as EGFR amplification.[13,4] The p16 tumor suppressor (encoded by CDKN2A) reduces the phosphorylation capacity of CDK4 and CDK6 cyclin-dependent kinases, therefore

allowing the G1 to S-phase transition in the cell cycle. Most glioblastomas with EGFR amplification show the p16 deletion as well.[13] The phosphate and tensin homologue (PTEN) mutation seen in 20% of glioblastomas causes downstream activation of the P13K/Akt/mTOR pathway, and therefore increases cell survival and proliferation.[19,20]

Proneural GBM often presents with increased expression of platelet-derived growth factor receptor (PDGFRA, PDGFR-α).[13] Platelet-derived growth factor encourages development and growth of connective tissues and glia. Two cell surface receptors (PDGFR-α and PDGFR-β) belong to the tyrosine kinase family, and PDGFR-α has been found to be involved in tumor proliferation. It has been found in low and high grade astrocytomas, and therefore is thought to be part of the proliferation and development at all stages. PDGFR-α amplification is only found in 16% of glioblastoma, but in most cases of secondary GBM.[13] Proneural GBM tumors are not only classified by increase PDGF-α, but also tumor suppressor (TP53) and retinoblastoma (RB) gene mutations.[4] TP53 is a transcription factor that activates genes and appears to act a stress-induced switch that can turn on arrested cell cycle in the G1 phase, or cause apoptosis. The TP53 mutation occurs in over 65% of secondary glioblastomas, but in less than 10% of primary GBM. The accumulation of the TP53 protein is more frequently observed than the actual gene mutation, and seen to be increasing in recurrent astrocytomas over time.[13] TP53 induces the transcription of the MDM2 gene (mouse double minute 2), and then MDM2 complexes with TP53, as a negative feedback mechanism to stop its transcriptional activity. Upregulation of MDM2 and the TP53-MDM2 complex formation can overcome the G1 checkpoint, and contribute to the alternative pathways for the cell to evade the TP53 regulated control of cell growth.[13] Previous research with adenovirus-delivered TP53 showed functional restoration of

the TP53 gene, leading to apoptosis in six glioma cell lines. Cellular proliferation was found to be inhibited in both *in vitro* and *in vivo* models, which resulted in prolonged survival in preclinical models.[21] More recently, interferon-B (IFN-B) has been found to sensitize T98G (GBM) cells to TMZ, thought to be a function of also being found to induce p53 overexpression.[22] The progression from low grade to high grade glioma is also associated with the blocked expression of the retinoblastoma (RB) gene, which serves to halt the cell cycle, therefore causing uncontrolled growth.[20]

A third, hybrid subtype of GBM called mesenchymal GBM exists, most commonly is found in younger patients. This GBM subtype is comparable to the primary GBM subtype in that it arises *de novo,* with no previous astrocytoma precursor occurrence, and about 30% PTEN mutation rate. It shares characteristics of secondary GBM, where both have greater than 30% rate of the TP53 mutation, and do not tend to occur in older adults.[13] It also presents with low expression or mutations of neurofibromin (NF-1), a gene related to a hereditary skin condition. A fourth subtype has been classified due to its lack of similarities with the previous three subtypes. Neural GBM presents with no outstanding genetic amplification or mutation rates, differentiating itself from the others.

**1.3 Current Treatment**

Currently, the standard method of treatment for GBM begins with maximal surgical resection of the tumor, followed by concurrent radiation and chemotherapy.[23] Because GBM penetrates surrounding tissues, surgical resection is unlikely to remove the tumor cells with comfortable margins, and further treatment methods must be used. Most often, a more recently approved drug, temozolomide ((8-Carbamoyl-3-methylimidazo(5, 1-d)-1, 2, 3, 5-

tetrazin-4(3H)-one), TMZ) is administered as a chemotherapeutic agent. Temozolomide is a prodrug that undergoes spontaneous hydrolysis into the active metabolite 5-(3-methyl)-1-triazen-1-yl-imidazole-4-carboximide (MTIC). This oral alkylating agent works by promoting methylation most often at the O6 position on guanine, initiating a sequence of DNA mismatch-repair events, leading to apoptosis [24,25]. TMZ has between 96 and 100% bioavailability when delivered orally, and was approved in 1999, since being the primary choice for GBM patients. It is usually administered at 75mg/$m^2$ daily with concurrent radiotherapy (RT) for 6 weeks, followed by 6 more weeks of a higher dosed TMZ, at 150 mg/$m^2$. Side effects include myelosuppression and nausea. The median overall survival with the described method remains at 14.6 months.[2]

The implantable chemotherapeutic was given great attention at the time of approval, in 1997. Carmustine (BCNU) had already been approved for systemic use, but the appeal of a local delivery system was justified through successful preclinical trials, and then clinical data.[8] Carmustine (BCNU) in the form of Gliadel ™ wafers are implanted into the resection cavity, to administer local cytotoxic drug to the GBM cells remaining after resection. BCNU is a nitrosurea, an alkylating drug working on the same pathway as TMZ, in which the polymeric wafers (poly carboxyphenoxy-propane/sebacic acid anhydride [PCPP:SA] wafers containing 3.85% BCNU) release BCNU for approximately 3 weeks.[26] Polymeric drug delivery has been an emerging approach to cancer treatment, where local delivery of controlled release systems can be used to allow for higher drug concentrations at the tumor site, as well as reduce toxic systemic effects[27]. At the time of development of polymeric delivery systems, carmustine (BCNU) was the most effective form of chemotherapy for gliomas, and thus chosen for local delivery. PCPP:SA wafers

have shown to allow for controlled sustained release and biodegradation via surface erosion. Using systemic free BCNU, patient cell counts can take weeks to recover before the next dose can be administered. These wafers allow for drug to be delivered over multiple days or weeks, in comparison to free BCNU, which has a half-life of 15-30 minutes.[8,27] Other drugs have been incorporated and tested in PCPP:SA wafers, including temozolomide, the current standard of treatment for GBM. TMZ impregnated wafers were even found to provide superior effects over oral delivery of TMZ in rodent glioma studies.[27] Though the Gliadel™ wafers have been proven effective in preclinical *in vivo* studies, treatment with the wafers does not significantly improve patient lifespan when translating clinically. Additionally, BCNU used for local delivery of chemotherapy has been said to produce high interstitial drug concentration, while data has shown minimal penetration of the resection cavity wall, to depths of approximately 1mm.[28] BCNU wafers are not currently used in many centers due to side effects such as delayed wound healing, intracranial edema and infection, CSF leakage and seizure, however are still generally regarded as safe.[2]

In addition, bevacizumab was approved for treatment of recurrent glioblastoma in 2009. Bevacizumab is a humanized monoclonal antibody that targets vascular endothelial growth factor (VEGF), and is also approved for use in other human tumors, such as non-small-cell lung cancer.[10] Progression of glioma growth has been shown to be mediated highly by tumor-associated blood vessels, and human glioblastomas have shown to overexpress angiogenic growth factors, compared with normal brain tissue.[29] A Phase II clinical study done, leading to approval, shows that bevacizumab as a single-agent has significant antiglioma activity, as well as significantly effecting the vascular permeability and decreasing cerebral edema.[30]

CHAPTER 2

BARRIERS TO TREATMENT & STRATEGIES TO OVERCOME BARRIERS

Various systemic drugs have been used as treatments in patients with GBM, several barriers to providing effective treatments remain, include crossing the blood-brain barrier (BBB) and chemotherapeutic resistance.

**2.1 The Blood-Brain Barrier**

It is estimated that less than 2% of small molecule drugs, and no large molecule drugs or genes will cross the blood-brain barrier (BBB).[28] The BBB exists to regulate transport of essential nutrients and to protect the brain from neurotoxins. It is a cellular barrier that regulates ionic concentrations to allow for synaptic signaling in the brain, while also preventing entry of cells and large molecules via tight junctions between endothelial cells.[11] Molecules can still cross the BBB through various mechanisms such as saturable transport, transmembrane diffusion, adsorptive endocytosis, and other extracellular pathways[31] (Banks, 2009). Most drugs have been found to cross the BBB through passive diffusion or saturable transport, dependent on physiochemical properties of substances including charge, molecular weight and hydrophobicity. Lipid soluble drugs with low molecular weight are favorable for diffusion, whereas water soluble drugs tend to transverse using transport proteins. However, various efflux transport systems exist to remove unwanted substances that traverse the BBB using passive diffusion. A largely studied efflux pump, P-glycoprotein (ABCB1, MDR1a), has been a persistent challenge in drug delivery due to its efficacy in removing small molecules from the brain.[31] A wide variety of ATP-dependent substrates are recognized by ABCB1, allowing for drug resistance to occur when these drugs are pumped out of cell through efflux pumps, reducing

cytotoxicity and drug efficacy.[32] In 1994, a knockout MDR1a mouse study found that P-glycoprotein is a major component of the BBB, after finding greatly increased administered drug concentrations specifically in the brain, compared with normal mice.[33] Inhibitors of the action of ABCB1 efflux proteins have been used clinically, where they have shown to allow for increased drug concentrations in some cases, but have failed to reverse multidrug resistance in solid tumors. Two products, elacridar and tariquidar, have been approved for use as ABCB1 inhibitors, but complete inhibition of ABC-transport proteins at the BBB is even more difficult than in other tissues.[11,34]

The BBB has been a consistent challenge in creating effective delivery systems for therapeutics. Nanotherapeutics currently in research are being designed with this challenge in mind, working towards creating targeted systems. However, all nanoparticles (NPs) currently approved are considered first generation NPs and rely on diffusion and passive targeting of tumor tissue via enhanced permeability and retention (EPR) effect.[35,36] Fenestrated capillaries exist in areas of rapidly and poorly grown vessels, due to increased VEGF expression and angiogenesis.[37,38] The leaky nature of the vasculature creates an interrupted BBB in the tumor, which should allow for an increase in drug or therapeutic concentration in the glioma tissue. However, it is possible that the leaky vasculature does not allow for therapeutically relevant increases in drug concentration. Séhédic et al. agrees that the EPR effect is unlikely to be efficient, due to the dense brain matrix and increased interstitial fluid pressure preventing diffusion.[39] Furthermore, glioma cells tend to easily travel outside the tumor to other normal regions of the brain. This metastasis not only makes the glioma more difficult to treat, but also

reduces the quantity of drug reaching tumor cells in the intact regions of the brain with perfectly functioning BBB.[11]

**2.2 Chemotherapeutic Resistance**

Glioblastomas have been found to have either inherent resistance to chemotherapeutic agents, or develop resistance during treatment. Drug resistance in GBM patients has been attributed in part to the (O)6-methylguanine-DNA-methyltransferase (MGMT) gene. The MGMT gene codes for the MGMT protein that removes alkyl adducts at the O(6) position of guanine, as a natural repair mechanism to prevents apoptosis due to DNA crosslinking.[40] Temozolomide promotes the addition of alkyl groups most frequently to the O(6) position of guanine, but also less often at the N(7)-guanine and N(3)-adenine positions, in order to cause DNA damage and programmed cell death.[25,41] The damage done from temozolomide is reversed or refuted due to upregulation of MGMT in GBM cells. Not only is MGMT upregulated due to the disease state, but it has been found that the TMZ mechanism of action causes inactivation of MGMT, which in turn leads to increased synthesis of MGMT protein *de novo,* in order to restore the natural DNA repair mechanism. TMZ, as well as

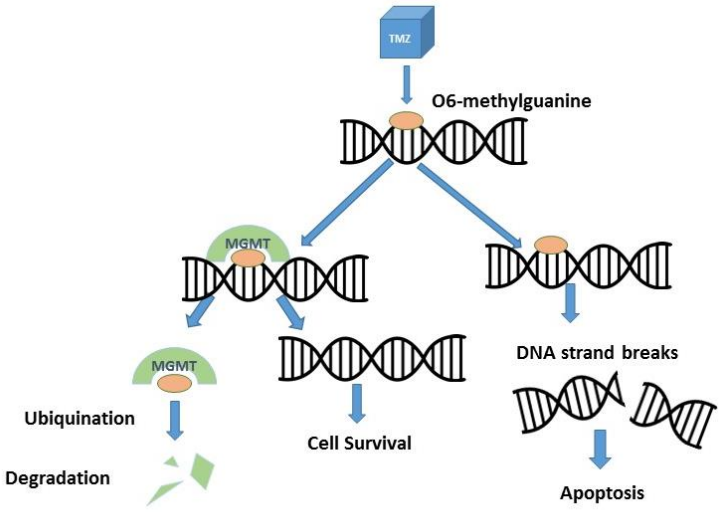


*Figure 3*. *Schematic of MGMT/TMZ mechanism*. TMZ, a DNA alkylating agent, methylates DNA at the O6 position on guanine, resulting in DNA damage and apoptosis. MGMT, a DNA repair protein, removes alkyl adducts from the O6 position of guanine.

other alkylating agents, have therefore been found to acquire a large amount of resistance when used for therapy, due to the cells upregulation of MGMT and their ability to respond to the TMZ-caused damages by further increasing MGMT production.[24] The restoration of MGMT by *de novo* synthesis occurs within hours, making the timing of TMZ dosing predictive of the therapeutic success.[24] A continuous TMZ dosing schedule increases the exposure and depletes MGMT optimally, reducing the possible resistance mechanism.[42] TMZ has also been found to induce EGFR amplification, a key agent in GBM formation, which allows for resistance development due to tumor progression during treatment.[43] Moreover, DNA lesions induced by TMZ are found to activate the p53 pathway, and patients with wild-type, rather than mutant p53 often found in secondary GBM, are found to respond more favorably to the treatment.[24]

Epigenetically, silencing of MGMT via promoter methylation has been found to be correlated with longer patient survival when treated with alkylating agents. Methylation of MGMT is only found to occur naturally in 30-60% of GBM cases.[25] In a retrospective study done by Donson et al., the inherent silencing of the MGMT gene provides better clinical outcomes for pediatric patients when treated with TMZ (P=0.007), but shows to more strongly correlate with longer patient survival regardless of treatment (P=0.0005), suggesting it may have more to do with tumor progression than just the resistance to TMZ.[44] Currently, attempts to overcome MGMT overexpression are being investigated by methods including using O6-benzylguanine as a pseudosubstrate for MGMT, and using RNA interference to silence the MGMT gene.[45,46]

Resistance occurs further due to poly(ADP-ribose)polymerase-1 (PARP-1), a base-excision-repair gene with activity that repairs lethal lesions (N7-guanine and N3-adenine) and repairs damage caused by TMZ. When PARP-1 is disrupted, cytotoxicity increases in response to

the methylation from alkylating drugs.[41] The PARP-1 gene has been shown to have increased activity in GBM cells treated with TMZ, likely in response to the DNA damage. Glioma stem cells also appear to play a role in chemoresistance in GBM. Glioma stem cells sampled from highly resistant GBMs express multidrug resistance protein-1 (MDR1), and at higher levels than do differentiated glioma cells. These non-differentiated stem cells therefore display more resistance to chemotherapeutic agents, such as TMZ, furthering the proliferation of the tumor.[47] Beier et al. explains that cancer stem cells can be intrinsically resistant, where treatment doesn't affect the tumor growth and recurrence is soon after treatment, or extrinsically resistance, where cancer stem cells survive in brain parenchyma and allow for distant recurrences.[48] These mechanisms together can allow for highly resistant and difficult to treat glioblastomas.

**2.3 Immunotherapy**

The research community has been addressing challenges in treating glioblastoma from many different angles. A few critical attempts have been in immunotherapy, gene therapy and various drug delivery modalities. Monoclonal antibodies have been researched for the purpose of inhibiting oncogene activity, and providing support to the body's immune system. Erlotinib, genfitinib, cetuximab, and bevacizumab have been used in phase II clinical trials to inhibit EGFR overactivity in high grade gliomas.[30,49–51] Results have shown that as single agents, these biologics are not effective in treating glioblastoma with the exception of bevacizumab, showing significant antitumor activity compared to historical controls.[30,52] Sorafenib has been researched in phase I clinical trials to inhibit PDGF receptor-b, with results proving safety.[53,54] However, one phase II trial that has been completed produced only 9% of patients with 6-month progression free survival, rendering sorafenib to have limited efficacy in treating GBM.[55] Pembrolizumab,

another immunotherapy, is in phase I/II clinical trials currently. It is used to inhibit the overexpressed programmed death ligand PD-L1 from providing protection to tumor cells in GBM patients, though results are not reported (NCT02530502). The increased expression of PD-L1 inhibits recognition and elimination by T-cells, and inhibition of this PD-L1 using pembrolizumab may assist the immune system in fighting off cancer.

### 2.4 Gene Therapy

Gene therapy includes both the delivery of genes to be integrated into the patients' cells, and the delivery genetic material to affect a patient's gene expression. The delivery of genes is traditionally to replace either missing or mutant genes to correct disorders, and can be delivered using viral or non-viral vectors. The delivery of genetic material regards using RNA interference (RNAi) to affect the expression of DNA and proteins,

#### 2.4.1 Viral Gene Delivery

Viral vectors have been studied and in clinical trials for years as delivery vehicles for genes into mammalian cells. The first clinical trial publishing gene therapy for glioma treatment used retrovirus-mediated HSV thymidine kinase (HSV-TK) and ganciclovir, beginning in 1992 (NCT00001328).[56,57] Certain viruses, considered neurotropic, have a tendency to interfere with and selectively bind with neurons and glial cells. These neurotropic viruses, such as HSV1, adenoviruses and paramyxoviruses have been specifically targeted as vectors for treatment of gliomas[58–60]. Various viral vector methods have been studied such as suicide gene therapy, which can be used to produce transcription enzymes that convert non-toxic prodrugs into lethal active compounds. Other virally transported gene therapy attempts include oncolytic, immunomodulatory and tumor suppressor gene therapy.[61] Phase III clinical trials done by Rainov

et al. tested the effects of combining retrovirus mediated herpes simplex virus-thymidine kinase gene (HSV-TL) with ganciclovir (GCV) in 248 patients with newly diagnosed GBM. The HSV-TK gene converts prodrug GCV to its active form GCV-triphosphate, to inhibit DNA replication and cell division of infected proliferative cancer cells. The group found that despite safety, low transfection efficiency in humans remains a challenge in producing significant differences in treatment groups (HSV-TK/GCV combined with chemotherapy and radiation) compared to those treated solely with chemotherapy and radiation.[62] Another clinical trial completed phase 2a in 2010, using adenovirus-mediated HSV- thymidine kinase (AdV/TK) therapy combined with anti-herpetic valacyclovir and radiation for the treatment of glioblastoma. Results showed that the treatment increased overall survival by 3.6 months compared to current standard of care.[63] Amphitropic retroviral replicating vector (RRV) Toca 511, developed by company Tocagen has their regimen in phase 2 clinical trials, where the Toca 511 virus infects and delivers the cytosine deaminase (CD) gene, and then orally taken Toca FC delivers fluorocytosine (FC) (NCT02414165). The CD enzyme produced allows for the FC prodrug to become an active anticancer drug (5-FU) and kill cancer cells, and has been concluded to be safe for intravenous administration in phase I trials. (NCT01985256).[64] Though viral vectors have been studied extensively, they have only resulted in marginal increase overall survival and have yet to achieve FDA approval after decades of study.

**2.4.2 Non-viral Gene Delivery**

Due to the inability to translate virally delivered therapeutics to market, many researchers have shifted focus to non-viral vectors. Recently, much research has gone into studying nanoparticles for the systemic delivery of drugs or genes. Nanoparticles (NPs) have

been of great interest for the delivery to the brain, with aims of crossing the blood brain barrier. They allow for conjugation of nucleic acids, homing peptides, or targeting ligands. Major types of nanoparticles used for delivery in glioblastoma include polymeric nanoparticles, liposomes and lipid nanoparticles.

*Polymeric nanoparticles*

Polymeric nanoparticles are widely studied due to their multifunctionality, and their ability to improve solubility, stability and biodistribution of therapeutics they carry.[65] They tend to be safer and more predictable than viral vectors. Aside from the array of naturally available polymers, there are endless possibilities in the field of synthetic polymers. The ability to create a nanoparticle to fit the biodegradation and drug-release profile needed for specific applications is appealing for drug and gene delivery alike. For delivery to brain tumors, polymeric NPs have potential capability to transport substances across the BBB. A few main types of polymeric NPs used for targeting glioblastoma include dendrimers, poly(β-amino ester) (PBAE) and polyethyleneimine (PEI).

Dendrimers are highly branched synthetic polymers that have been used for the delivery of nucleic acids, specifically siRNAs. They also have the ability to incorporate drug delivery or imaging agents for additional therapeutic benefit. Poly(amidoamine) (PAMAM) dendrimers have been of interest because they can conjugate with siRNAs and targeting ligands such as folic acid for increased delivery specificity, and have been found to cross the BBB. A study by Waite et al. conjugated cyclic RGD (arginine-glycine-aspartic acid) peptide to PAMAM dendrimers, as a targeting moiety to cellular integrins. They then conjugated siRNAs to the complex and delivered to U87 glioma cell spheroids, with findings that their delivery system was able to penetrate

malignant spheroids and efficiently produce gene silencing.[66] One critical limitation of PAMAM dendrimers for clinical translation is cytotoxicity due to their high positive surface charge. Studies have shown that PAMAM dendrimers exhibit neurotoxicity by inducing autophagy in glioma cells resulting in cell death.[67] Strategies to mitigate this effect include reducing the surface charge through acetylation or functionalization using PEG.

One group used a poly(β-amino ester) nanoparticle conjugated with DNA coding for the herpes simplex virus-thymidine kinase gene (HSV-tk), and ganciclovir (GCV) for therapy in glioma cell lines. They found that the cell lines (9L and F98) *in vitro* had 100% cytotoxicity compared the cells transfected with green fluorescent protein (GFP), an innocuous gene, and also treated with GCV. When delivered *in vivo,* they found that glioma-bearing rats had a significant survival benefit over control rats.[68] Another group used the biodegradable PBAEs conjugated to DNA and achieved over 60% transfection in human brain tumor initiating cells (BTICs) in nude mice, and significant specificity for transfection in tumor tissue over normal brain tissue. PBAEs show promise as a non-viral vector for genes in brain tumors, with lower immunogenicity and higher transfection efficiency.[69]

Polyethyleneimine (PEI) is another commonly used synthetic nanoparticle that can effectively complex with nucleic acids, such as siRNA and DNA. PEI is a cationic polymer that can be modified with hydrophobic polymers or targeting ligands for combination drug delivery or targeted delivery, respectively. PEI can easily penetrate the cellular membrane, and escape the endosome using proton buffering. Additionally, to reduce the cytotoxic effect of PEI and enable attachment of targeting ligands, poly(ethylene glycol) (PEG) conjugation is commonly applied to PEI. RGD ligands and PEG have been conjugated to PEI for the delivery of plasmid DNA. Zhan et

al. found that this complex allowed for efficient gene transfection in U87 glioma cells *in vitro* and *in vivo.*[70]

*Cationic liposomes and lipid nanoparticles*

Liposomes have been studied extensively as a non-viral vector for the use of drug and gene delivery. Cationic lipids tend to electrostatically complex with DNA to form positively charged lipoplexes.[71,72] Though gene delivery via liposomes has been accepted as safe, liposomes have not proven highly effective for gene transfection in humans. However, liposomes have the ability to carry hydrophobic or hydrophilic molecules within their vesicular structure, making them good vehicles for drug delivery. In delivery to tumors, it has been found that cationic liposomes accumulate in tumor tissues due to their positive charge. To deliver across the BBB to brain tumors, one group used focused ultrasound to deliver doxorubicin loaded cationic liposomes (DOX-CLs), and then allowed DOX-CL to target C6 glioma tissue *in vivo*. They found that the delivery system increased animal survival time and decreased progression of glioma growth, compared with free DOX.[73] A study by Calcagno et al. developed a cationic liposome (scL-TMZ) for the delivery of TMZ to glioblastoma cells (U87R). They found that the liposome increased the sensitivity of resistant cells to TMZ treatment compared to when treated with free TMZ.[74] The only synthetic nanomedicine to reach clinical trials for systemic delivery to data are cationic liposomes.[61]

Solid lipid nanoparticles have been in laboratories since the 1990's, and are studied in delivery to the brain in part due to their hydrophobic, low molecular weight characteristics, making them favorable for transport across the BBB.[11] Lipid NPs have advantages over other delivery systems, such as good biocompatibility, controlled drug release and minimal

cytotoxicity. They also have the ability to deliver otherwise highly insoluble lipophilic drugs across the BBB.[75] Nanostructured lipid carriers (NLCs) are composed of solid and liquid lipids, allowing for greater drug loading due to an imperfect crystal structure. A study by Chen et al. loaded TMZ and pGFP into NLCs (made from soya lethicin, DDAB and tween 80), to determine feasibility in delivering drug and gene through the mouse tail-vein to human glioma tumors (formed subcutaneously with U87 cells). They found significant increase in gene transfection compared to positive control Lipofectamine 2000, and significantly increased cytotoxic effect compared with free TMZ.[76] One group investigated the ability of polymeric NPs, solid lipid NPs and nanostructured lipid carriers to deliver TMZ to glioblastoma tumors. They developed each nanoparticle to be loaded with TMZ and evaluated the anti-tumor activity *in vitro* and *in vivo,* and found that the nanostructured lipid carriers displayed the most significant glioma growth inhibition.[75]

### 2.4.3 RNA interference

RNA interference (RNAi) has become the gold standard for the silencing of genes since its discovery in 1998.[77] RNAi can be achieved by using plasmid DNA (pDNA), small hairpin RNA (shRNA) or short interfering RNA (siRNA). MicroRNAs (miRNAs) are another interference method used, similar to siRNA in length and non-coding nature, but lacking the limited specificity to one mRNA. Most commonly focused on for gene silencing is siRNA, due to its specificity and proven safety and efficacy.[78] Interference occurs when the antisense siRNA will bind to a target mRNA to induce nucleolytic degradation of a specific gene, and prevent translation of a desired protein. In cancer, siRNAs have been found to be useful in silencing proliferative genes, or oncogenes, that allow for uncontrolled growth of tumors, as well as showing promise in

sensitizing cancer cell to chemotherapeutics.[78] Initially, local delivery of siRNAs to the tumor was relied on for therapeutic effect, however research has progressed in creating delivery systems to protect the siRNA stability from degradation by nucleases in the body using carriers such as gold nanoparticles, polymeric micelles and liposomes.[77] Specificity and efficiency of siRNA have been proven *in vitro, in vivo* and through clinical trials, but not without unwanted effects such as nonspecific inflammation and challenges such as siRNA instability and producing controlled siRNA release from the delivery vessel.[77] Yoo et al. has researched an iron oxide nanoparticle conjugated chlorotoxin peptide (CTX) for targeting GBM cells (T98G) and to siMGMT for silencing MGMT. They found that their nanoparticle increased sensitivity to TMZ and cytotoxicity *in vitro* and *in vivo*, but were unable to distinguish if this effect was due to CTX or the MGMT silencing.[79] Wang et al. published work delivering siRNAs to silence EGFR and β-catenin in GBM cells (U-87 MG), where they found that cell proliferation was reduced when treated with siRNAs targeting β-catenin and β-catenin + EGFR, but not EGFR alone.[52] Clinical trials using siRNAs are few, with only a handful attempted for the treatment of tumors. Clinical trials administering siRNAs for the direct silencing of genes for GBM treatment have yet to be attempted.[80,81] The use of RNA interference can be very valuable in reducing the expression of genes and proteins in certain cells, rather than introducing new or improved genes into the genome.

**2.5 GBM Treatments in Clinical Trials**

Previously discussed therapies in clinical trials, as well as additional treatments for glioblastoma currently in clinical trials are displayed in Table 1. Most treatments in clinical trials currently are virally delivered gene therapies, combined with cytotoxic drugs. However,

therapies include a vaccine, neural stem cell injections, and an MGMT pseudosubstrate. A survivin peptide vaccine (SurVaxM) treatment is currently in clinical trials with attempts to treat gliomas by eliciting an immune response to the overexpressed survivin protein in GBM cells. In phase 2 trials, SurVaxM has been used in combination with TMZ, Sargramostim, and Montanide ISA 51 VG, in order to kill cancer cells, restore blood cells suppressed due to the therapy, and as an adjuvant to human vaccine, respectively. (NCT01250470)[82,83] *In vivo* studies show that siRNA knockdown of survivin induces apoptosis in GBM tumors and significantly inhibits glioma growth.[84]

A phase I clinical trial implanted neural stem cells (HB1.F3) expressing E. coli cytosine deaminase (CD) into the resection cavity of high grade glioma tumors. Oral 5-fluorocytosine (5-FC) was given, with the intent of the expressed CD enzyme to convert 5-FC to the lethal compound 5-FU. This first in man study concluded safety and feasibility to target brain tumors, as well as produce a local cytotoxic effect (NCT01172964).[85] Phase II clinical trials are currently recruiting recurrent GBM patients for the study of SGT-53, a cationic liposome encapsulating wild-type p53 tumor suppressor gene in a plasmid backbone, in hopes that the delivery of normal p53 gene in combination with TMZ will provide longer overall survival (NCT02340156). SGT-53 has shown promise in mice, where sensitivity to TMZ was shown to be enhanced with treatment.[86] $O^6$-benzylguanine ($O^6$-BG) was developed as a substrate inhibitor of MGMT, working by binding to MGMT and diminishing the enzyme activity. $O^6$-BG has been and is still in clinical trials, in combination with alkylating agents TMZ and BCNU, and has shown thus far to increase sensitivity of the tumors to the alkylating agents.[45] A phase II clinical trial has been completed using $O^6$-benzylguanine in combination with temozolomide in pediatric patients with

high-grade gliomas, and it was concluded that the combination did not achieve the target therapeutic response rate.[45,24] However, another phase II clinical trial of TMZ plus O-6BG in adults concluded that the combination restored sensitivity to TMZ.[87]

| VECTOR | MAIN THERAPEUTIC AGENT | MECHANISM | COMBINATION | CLINICAL TRIAL PHASE | REFERENCES |
|---|---|---|---|---|---|
| Liposome | SGT-53 | Introduce wild-type tumor suppressor p53 gene to sensitize cells to TMZ | TMZ (chemotherapeutic) | Phase II | NCT02340156[86] |
| Retroviral Replicating Vector | Toca 511/ Toca FC | Introduce yeast cytosine deaminase (CD) gene to convert prodrug 5-FC to lethal compound 5-FU | Oral 5-FC (cytotoxic) | Phase II | NCT02414165[64] |
| Adenovirus | AdV/tk | Herpes thymidine kinase delivered to cancer cells, then anti-viral valacyclovir targets expressing cells | Valacyclovir (anti-viral) | Phase IIa | NCT00589875 [63] |
| Adenovirus | Recombinant adenovirus-p53 SCH-5850 | Introduce wild type tumor supressor p53 gene into brain cells, into resection cavity | Conventional surgery | Phase I | NCT00004080 [88] |
| Retrovirus | MGMTP140K-encoding retroviral vector | Genetically modified peripheral blood stem cells may prevent side effects (myelosuppression) from chemotherapy as O6-benzylguanine prevents TMZ resistance caused by MGMT overexpression | -O6-benzylguanine (MGMT inhibitor)<br>-TMZ (chemotherapeutic)<br>-Radiation | Phase I | NCT01269424 |
| Neural Stem Cell | HB1.F3 | Neural stem cells expressing E. coli cytosine deaminase (CD) gene implanted into resection cavity and prodrug 5-FC is converted to lethal 5-FU | Oral 5-FC (cytotoxic) | Phase I | NCT01172964 |
| Vaccine | SurVaxM | Survivin vaccine causes body to elicit immune response to cells expressing survivin | -Sargramostim (biological)<br>-TMZ (chemotherapeutic)<br>-Montanide ISA 51 VG (drug) | Phase II | NCT02455557, [82] |
| MGMT pseudo-substrate | O(6)-benzylguanine | O(6)-BG irreversibly inactivates MGMT in order to improve effectiveness of TMZ | TMZ (chemotherapeutic) | Phase II | NCT00275002, [87] |

*Table 1. Current state of clinical trials for the treatment of glioblastoma multiforme.*

CHAPTER 3

RESEARCH AIMS

## 3.1 Objectives

The current treatment options for glioblastoma do not effectively improve the disease, and great improvement is needed to extend patient lifespan. The overall goal of this research is to develop a multifunctional nanotherapeutic for the treatment of malignant glioblastoma. It is hypothesized that combinatorial delivery of temozolomide and siRNA targeting MGMT will sensitize tumor cells to TMZ, a DNA alkylating agent, due to the knockdown of MGMT. This study will focus on nucleic acid delivery for the future combination treatment with TMZ.

## 3.2 Multifunctional Nanotherapeutic Design

The polymeric micelle PgP, or poly(lactide-co-glycolide) -graft-polyethyleneimine, is a novel polymeric system developed by our lab, with the potential to deliver nucleic acids and drugs. The cationic, amphiphilic copolymer assembles spontaneously into micelles in an aqueous environment. As represented in Figure 4, the hydrophobic PLGA constructs the core, and the positively charged polyethyleneimine (PEI) makes up the shell of the micelle. PgP is designed to

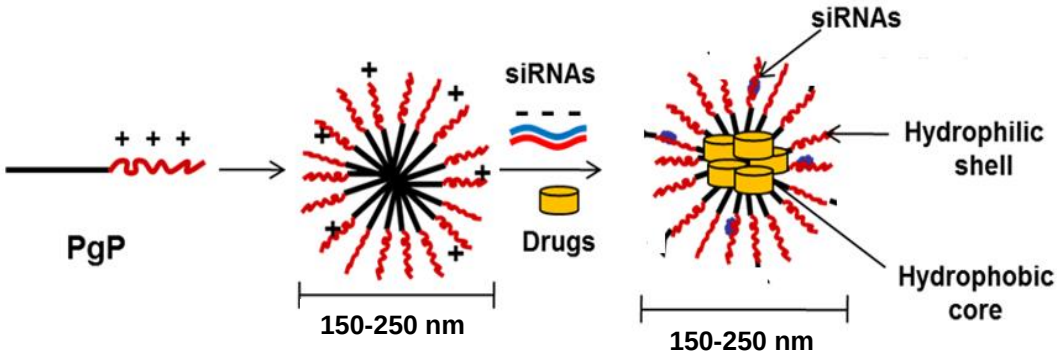


*Figure 4. PgP micelle schematic.* The micelle formation of poly(lactide-co-glycolide)-graft-poly(ethylenimine), PgP. Hydrophobic PLGA orients into the core and the hydrophilic PEI orients to the shell of the micelle formation. The cationic polyplex then allows for delivery of both drug and siRNA for maximum therapeutic effect.

be complexed with negatively changed nucleic acids to form a polyplex held together with strong electrostatic interaction between the nucleic acids (such as siRNA) and the PEI shell. The hydrophobic core allows hydrophobic or lipophilic drugs to be loaded within for delivery. The approximately 200nm polyplex is strategically between the sizes of kidney and liver excretion, designed to allow the polyplex to avoid clearance and stay in circulation when administered intravenously. When the polyplex enters circulation, it can be targeted to cancerous tumors via the enhanced permeability and retention (EPR) effect, as described previously. Once the polyplex makes its way into the tumor cell, it can be taken up into the cell via endocytosis, and escapes by means of the proton sponge effect. Due to the cationic nature of the polyplex, the endosome will swell in attempt to maintain homeostasis, and eventually rupture, allowing the contents to release into the cytosol, and siRNA to escape.

**3.3 Study Design**

Determining efficacy of this polyplex includes determining the stability of the PgP when conjugated with siMGMT. Once the stability is determined *in vitro,* the cytotoxicity of the polyplex in human glioblastoma (T98G) cells will be assessed. The efficacy of siRNA delivery, as well as the reduction in gene expression and protein production will be evaluated *in vitro.* The stability of the polyplex will be evaluated by presenting the polyplexes to various physiological-like conditions *in vitro,* such as serum and ribonucleases. Given the polyplex is proven stable in physiological conditions, the cytotoxicity is minimal, and the polyplex proves effective in siRNA delivery, the delivery system will be introduced to mice, for *in vivo* studies of efficacy. *In vivo* studies first involve producing a xenograft glioblastoma model. This will involve introducing T98G cells, as studied *in vitro,* into the brains of nude mice. Determination of the tumor growth

can be made with analysis of the brain tissue *ex vivo,* on the macroscopic and microscopic levels. Confirmation of tumor cell growth within the mice can allow this project to move forward to studies of the polyplex biodistribution and therapeutic efficacy. Therapeutic efficacy of PgP/siMGMT will be evaluated in mice by injecting polyplex to the tumor site, then removing tumor tissue for protein and RNA extraction. Comparing untreated control tumor tissue with treated tissue will allow knockdown efficiency *in vivo* to be analyzed. Future studies can include assessing the antitumor effect of MGMT knockdown when combined with TMZ.

CHAPTER 4

MATERIALS & METHODS

## 4.1 Materials

Poly(lactide-co-glycolide) (PLGA, 4KDa 50:50) was obtained from Durect Corporation, Pelham, AL. with a carboxylic end group and 25 kDa branched polyethyleneimine (bPEI) was purchased from Sigma-Aldrich, St. Louis, MO. All siRNAs were purchased from GE Healthcare Dharmacon (Lafayette, CO). siRNA targeting MGMT (O6-methylguanine-DNA methyltransferase, NCBI Reference Sequence: NM_002412.4, siMGMT) was custom-synthesized. siGENOME non-targeting siRNA #5 (siNT) was also purchased and used as a negative control siRNA. Additionally, siNT with a fluorescein label (FI-siNT) at the 3' end of the anti-sense strand was synthesized and used in fluorescence experiments. The T98G cell line was obtained from ATCC in Manassas, VA. LysoTracker™ Blue DND-22 and Mouse monoclonal anti-MGMT antibody (clone MT3.1), Halt™ Protease & Phosphatase Inhibitor Cocktail, Pierce BCA protein assay kit, SuperSignal™ West Pico Chemiluminescent Substrate, and the cDNA Reserve Transcription Kit were obtained by Fisher Scientific. Mouse monoclonal anti-β-actin antibody (1:5,000) was obtained from Santa Cruz Biotechnology, Dallas, TX. Goat anti-mouse secondary antibody was obtained from Southern Biotechnology, Birmingham, AL. Immun-Blot® PVDF membranes were obtained from Bio-Rad Laboratories, Hercules, CA. Phenylmethanesulfonyl fluoride and Thiazolyl blue Tetrazolium Bromide (TBTB) were obtained from Sigma-Aldrich. Taqman® Gene Expression Assays Thermo Fisher Scientific, Waltham, MA. Nude athymic mice (Foxn1$^{nu}$) were obtained from Envigo. Buprenorphine was obtained from Hospira, Inc. Hamilton syringes were obtained from Hamilton

Company, Reno, NV. Nucleospin RNA/Protein kit was obtained from Machery-Nagel, Bethehem, PA.

**4.2 Synthesis of poly(lactide-co-glycolide)-graft-poly(ethyleneimine)**

The cationic, amphiphilic copolymer poly(lactide-co-glycolide)-g-polyethyleneimine (PgP) was synthesized as previously described [89] using 4 kDa poly(lactide-co-glycolide) (PLGA, 50:50) with a carboxylic end group and 25 kDa branched polyethylenimine (bPEI). PgP was purified using a dialysis membrane with molecular weight cut-off (MWCO) of 50,000 Da. PgP was then centrifuged at 5,000 rpm for 10 minutes in order to remove excess PLGA precipitate, and lyophilized for storage.[89]

**4.3 Gel shift assay**

In order to determine the optimal N/P (amine: phosphate) ratio necessary for complete binding of the PgP and free siRNA complex, a gel shift assay was performed. A 2% agarose gel was prepared with a 12-well comb. PgP was complexed with siRNA in deionized water at various N/P ratios ranging from 0 to 25 and incubated for 30 minutes at 37°C. Loading dye was added to the samples and each was loaded into the gel, then samples were electrophoresed at 100V for 25 minutes. It was stained with 0.2% ethidium bromide in water for 10 minutes and then rinsed with water for 15 minutes on a shaker. The ChemiDoc-It$^{2}$™ system was used to image the gel using an ethidium bromide filter and UV light (UVP, Upland, CA).

### 4.4 Characterization of PgP/siMGMT

To evaluate the particle size and surface charge of polyplexes, PgP was complexed with siMGMT (20 μg) at N/P ratio of 30:1 and 60:1. The N:P ratios were identified from gel shift assay. The polyplex was measured in using a Zetasizer (Malvern Zetasizer ZS DLS-Zeta) instrument that measured particle size, polydispersity index (PDI), and surface charge (zeta potential).

### 4.5 Cell culture

The human glioblastoma cell line T98G was cultured in specified growth media supplemented (EMEM) with 10% fetal bovine serum (FBS) and 1% antibiotic (100IU/ml penicillin/100μg/ml streptomycin), and grown in an incubator at 37°C with 5% $CO_2$.

### 4.6 PgP-mediated MGMT silencing

The efficiency of siMGMT transfection and MGMT silencing was quantified in T98G cells. Polyplexes were formed by complexing PgP with siMGMT (100 nM) at N/P ratios of 30:1, 60:1, and 80:1 in sterile deionized water at 37°C for 30 min. siMGMT complexed with Lipofectamine 2000 was used as a positive control. Additionally, at each N/P ratio, siNT was complexed with PgP as a negative control for comparison of each treatment. T98G cells seeded at $1x10^5$ cells per well and cultured in 12-well plates were washed three times with media and incubated with PgP polyplexes for 24 hours in media containing 10% FBS, after which, cells were again washed three times with media and incubated with complete media containing 10% FBS for another 24 hours. 48 hours post-transfection, protein or RNA was extracted from the cells for western blot or real-time PCR analyses, respectively, as described in the following sections.

To analyze the knockdown of MGMT on the protein level, western blot was performed. 48 hours post-transfection, cells were washed with 1X cold PBS and lysed with ice cold RIPA buffer (50 mM Tris-HCl, pH 7.4, 150 mM NaCl, 0.5% sodium deoxycholate, 0.1% SDS, and 1% NP-40)) containing protease inhibitor, phenylmethanesulfonyl fluoride and Halt™ Protease & Phosphatase Inhibitor Cocktail. Total protein concentration was determined using the Pierce BCA protein assay kit via the manufacturer's instructions. 3 µg of protein lysates were resolved by SDS-PAGE using polyacrylamide gels and transferred onto Immun-Blot® PVDF membranes. PVDF (polyvinylidene fluoride) membranes were blocked for 1 hour in Tris-HCl-buffered saline containing 0.1% Tween-20 (TBS-T) and 5% milk. Following blocking, membranes were incubated with mouse monoclonal anti-MGMT antibody (1:500) or mouse monoclonal anti-β-actin antibody (1:5,000) overnight at 4°C then washed four times with TBS-T and incubated in horseradish peroxidase-conjugated goat anti-mouse secondary antibody (1:2,000 or 1:10,000) for one hour. SuperSignal™ West Pico Chemiluminescent Substrate (Fisher Scientific) was used to detect immunoreactive bands which were subsequently imaged using the ChemiDoc-It$^{2}$™ Imager.

To analyze MGMT knockdown on the mRNA level, RT-PCR was used. After 48 hours transfection, total RNA was extracted from cells using the RNeasy® Plus Mini Kit (Qiagen, Valencia, CA) according to the manufacturer's instructions. The concentration and purity of isolated RNA was determined using the Biotek plate reader and Take3 Micro-Volume Plate. Isolated RNA (100 ng) was reverse-transcribed using the High-Capacity cDNA Reserve Transcription Kit with MultiScribe® Reverse Transcriptase (RT) and RT Random Primers. Real-time PCR was performed using a Rotor Gene Q thermal cycler (Qiagen) with predesigned

Taqman® Gene Expression Assays for MGMT (Hs01037698_m1), and the endogenous control, 18S (4319413E), combined with Taqman® Gene Expression Mastermix according to the manufacturer's instructions. The threshold cycle ($C_T$), the cycle number at which the fluorescence generated within the reaction crosses the threshold line, was determined. Relative mRNA expression of MGMT was calculated using the $2^{-\Delta\Delta}C_T$ method. Minus RT reactions were also performed to ensure that there was no significant genomic DNA contamination.

**4.7 Cytotoxicty of PgP/siMGMT**

To evaluate if the polyplex caused toxicity to the cells, a cytotoxicity study was performed. T98G cells ($1X10^5$ cells/well) were cultured in 24-well plates and allowed to attach overnight. PgP polyplexes were formed using siNT (100nM) at N/P ratios of 30:1, 60:1 and 80:1, incubated at 37°C for 30 minutes. Controls consisted of untreated cells, siNT alone, and Lipofectamine2000/siNT. Polyplexes were incubated with T98G cells for 24 hours in media containing 10% FBS, and then washed three times with media and incubated for an additional 24 hours. At 48 hours post-transfection, an MTT assay was performed to determine cytotoxicity. Cells were incubated with 120 µL/well of Thiazolyl blue Tetrazolium Bromide (TBTB) dissolved in PBS at 2 mg/ml, added to 500µL media. After a 4 hour incubation at 37C, the media containing TBTB was aspirated and 500µL DMSO was added to each well to dissolve formazan crystals. Wells were thoroughly mixed using micropipette and 100µL from each sample was removed and transferred into a 96-well plate. The Biotek Synergy plate reader (Winooski, VT) was used to measure absorbance of wavelength of 570 nm in order to determine concentrations of formazan in each well. Samples were normalized using untreated cells, and cell viability was determined using following equation: Cell viability (%) = $(OD_{570(sample)}/OD_{570(control)})$ x 100%.

### 4.8 Stability of PgP/siRNA polyplexes in various conditions

#### 4.8.1 Heparin competition assay

To determine the stability of the PgP/siRNA polyplex, polyanion heparin was introduced to the polyplex. First PgP/siRNA polyplexes were formed at an N/P ratio of 60:1 and incubated for 30 minutes at 37°C. Then heparin was added to the samples at various weight ratios (heparin: siRNA) and incubated for 30 additional minutes. Control groups of siRNA alone and PgP/siRNA without heparin were included. Weight ratios included 1, 2, 5, 10, 20, 50 and 100. Conditions described previously were used to run the gel with 20 uL of each sample was loaded.

#### 4.8.2 Serum and RNase protection assay

The stability of the polyplexes in the presence of serum and RNase were tested and compared to the stability of the polyplex in water. PgP/siRNA was also compared to negative control of siRNA alone, and known transfection reagents PEI and Lipofectamine® 2000 (LIPO). PgP/siRNA was complexed at N/P 60:1 in water for 30 minutes at 37°C; PEI/siRNA was complexed at N/P 5:1 in water and incubated for 30 minutes; LIPO/siRNA was complexed in Opti-MEM at manufacturer suggested N/P; and naked siRNA was prepared in water.

Samples were next exposed to 10% serum, 50% serum, or 0.1 µg RNAse A conditions and incubated 1 hour at 37°C. After incubation, 10% SDS was used to dissociate the siRNA from complexes, and samples were immediately run through gel electrophoresis using above described conditions. Each sample was compared to a respective control where the serum or RNAse conditions were replaced with a 30-minute incubation in water. The samples were

examined by gel electrophoresis using a 2% agarose gel stained with ethidium bromide and imaged with the ChemiDoc-It$^{2}$™ Imager.

**4.9 PgP-mediated intracellular uptake of siRNAs**

Transfection efficiency using PgP as a delivery system was tested by first transfecting T98G cells with fluorescently labeled siRNA (FI-siNT) and observing using fluorescent microscopy. T98G cells were seeded in 12-well plates at 1X10$^{5}$ cells per well and allowed to attach overnight. PgP was complexed with FI-siNT (100 nM), a fluorescein non-targeting siRNA, at N/P ratios of 30:1, 60:1, and 80:1 and incubated for 30 minutes at 37°C. FI-siNT alone was used as a negative control and FI-siNT complexed with PEI (5:1) or Lipofectamine 2000 were used as positive controls. Media (EMEM + 10% FBS) was added to each sample and then 1 mL was added to each well. Each well contained 2 µg siRNA. After 6 hours, cells were washed three times with 1X phosphate buffered saline (PBS) and transfection efficiency was evaluated based on density and brightness of cell fluorescence using confocal microscope. To examine the uptake mechanism of polyplexes, cells were stained with LysoTracker™ Blue DND-22 according to the manufacturer's instructions prior to imaging.

For quantitative analysis, flow cytometry via the Guava Easycyte ™ (Millipore, Darmstadt, Germany) was used to determine transfection efficiency. Cells were trypsinized and removed from well plates, and each sample was run through the flowcytometer. Cell populations were gated according to fluorescence of untreated cells. A heparin wash was used to ensure that fluorescently labeled siRNA was in fact entering the cells, rather than adhering to the cell surface.

**4.10 Effect of MGMT knockdown on antitumor activity of TMZ**

To evaluate the effect of MGMT knockdown on the cytotoxicity of TMZ, combination treatment was performed. T98G cells were plated at $1X10^5$ cells per well in 24-well plates and allowed to attach overnight. PgP/siMGMT polyplexes were made at N/P ratio 60:1 and incubated for 30 minutes. Polyplexes were added to the cells, immediately followed by TMZ addition at concentrations of 500 μM (half the IC50 value) and 1000 μM (IC50). MTT assay was performed 72 hours after transfection. Untreated cells were used as a control. Free TMZ, PgP/siNT with TMZ, and PgP/siNT or PgP/siMGMT without TMZ were used for comparison

**4.11 Generation of xenograft glioblastoma model in athymic mouse brain**

All animal procedures were conducted according to NIH guidelines for the care and use of laboratory animals (NIH publication No. 86-23, revised 1996) and approved by the Clemson University Animal Research Committee (animal protocol number AUP 2016-080). Eight week-old nude female athymic mice were used to create a GBM brain tumor model. Mice were anesthetized using isofluorane gas and were arranged into a stereotactic frame. Buprenorphine (0.1 mg/kg) was injected subcutaneously for pain before incision. An incision was made along the sagittal plane on the scalp, the bregma was located and the point 1.5 mm to the right was marked. A 26-guage Hamilton syringe containing 4μL of T98G cells, a total of 150,000 cells, was assembled into the stereotactic frame and inserted 3 mm deep into the brain. The cells were injected at a controlled flow rate of 1 mL/min and then the syringe was allowed to remain in the injection site for 5 minutes before removal. The syringe was slowly removed and sterile bone wax sealed the hole in the skull and the incision site was sutured.

**4.12 Biodistribution of DiR-loaded polyplexes after intratumoral injection**

We first evaluated the biodistribution of polyplexes to determine whether polyplexes remain in the tumor or diffuse out after intratumoral injection. To visualize the polyplexes, DiR was loaded into PgP using solvent evaporation method. Two weeks post-injection of tumor cells, mice were treated with with DiR-loaded polyplexes (DiR-PgP/siNT) for biodistribution analysis. Using the procedure previously described, mice were anesthetized, arranged in stereotactic frame, and injected with DiR-PgP/siNT, containing 2μg siRNA and 4μL volume. The injections were performed at the same original injection site (1.5 mm right of bregma, 3mm deep) at a flow rate of 1μL/min. Mice were imaged at 1 hr, 3 hr, 6 hr, 24 hr, and then every 48 hours for 10 days. Live animals were anesthetized using isoflurane and placed into the IVIS Luminar XR *in vivo* imaging system (Caliper Life Science). An excitation wavelength of 745nm and emission of 790nm was used to image the DiR loaded polyplex, to analyze the biodistribution of polyplexes. At day 10, mice were euthanized and organs were extracted for *ex vivo* analysis of the complex retention in tissues.

**4.13 Knockdown efficiency of PgP/siMGMT after intratumoral injection in athymic GBM model**

For knockdown efficiency analysis, mice were treated with siNT or siMGMT (2 μg, 4 μL volume) complexed with PgP, four weeks post-injection of tumor cells. Using the procedure previously described, mice were anesthetized, arranged in stereotactic frame, and injected with PgP/siNT or PgP/siMGMT, containing 2μg siRNA and 4μL volume. The injections were performed at the same original injection site (1.5 mm right of bregma, 3mm deep) at a flow rate of 1μL/min. Mice were euthanized 72 hours post-treatment and the brain was excised and preserved in RNAlater. A 1mm x 1mm x 2mm sized tissue sample was taken from each brain at the same location, in

order to remove tumor tissue. RNA and protein was extracted using Nucleospin RNA/Protein kit according to the manufacturer's instructions. Following extraction, the RNA purity and concentration was quantified using the Take3 plate reading system. The protein concentration was quantified by performing BCA assay, and protein was analyzed using western blot, using the methods previously described. The MGMT mRNA expression was evaluated by performing reverse transcription and then RT-PCR, as described previously.

**4.14 Statistical Analysis**

Quantitative data were presented as mean ± SEM. Statistical analysis was performed using either Student's t-test or one-way ANOVA (Bonferroni's Multiple Comparison Test). A value of $P<0.05$ was considered statistically significant. All statistical analyses were examined using GraphPad Prism 6 software.

CHAPTER 5

RESULTS

**5.1 PgP effectively binds siRNAs**

The amphiphilic, cationic micelle PgP was designed to self-assemble with a hydrophobic PLGA core, and a positively charged PEI shell, for the formation of a polyplex when bound with nucleic acids. This gel shift assay was performed in order to determine the effective binding amine: phosphate (N/P) ratio for PgP and siRNA. The PgP/siRNA polyplex was found to bind with stability at N/P ratios over 15:1 (Fig. 5), where there was no detectable unbound siRNA in the gel. Free siRNA suggests unstable or lack of binding with the PgP. A noticeable reduction in free siRNA, and therefore a noticeable increase in bound siRNA is seen starting at an N/P of 7.5. This finding allowed us to choose N/P ratios over 15:1 to continue forward with. In our previous study published in Biomaterials, we found that PgP/siRhoA at N/P 30:1 showed efficient knockdown in B35 cells, as well as rat spinal cord injury model *in vivo*[89]. These finding lead us to choose ratios, above 30:1 (30:1, 60:1 and 80:1) for further experimentation.

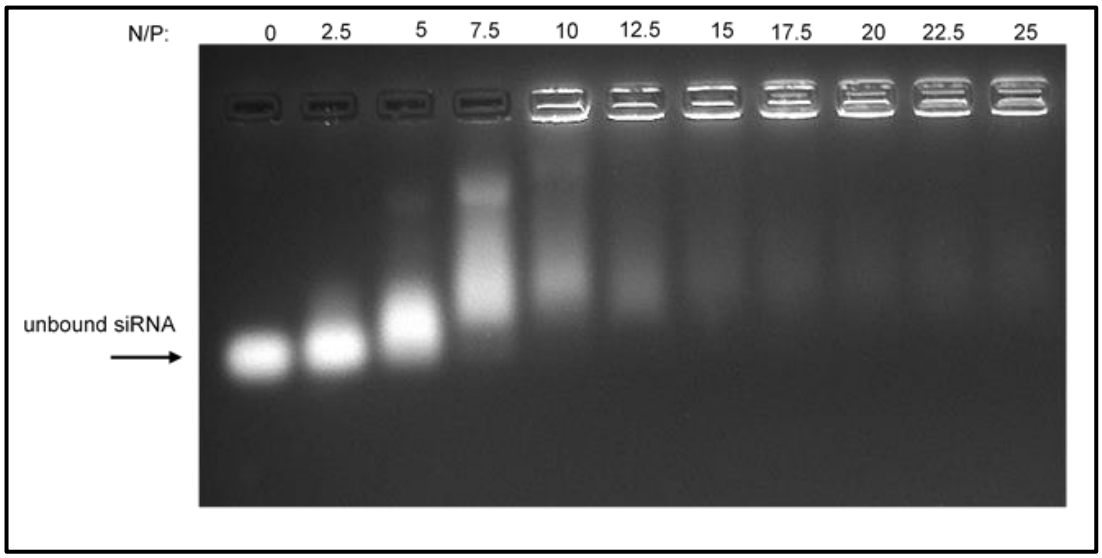


*Figure 5. Agarose gel shift assay of PgP complexed with siRNA*. PgP binds siRNAs at various N/P ratios, with greatest stability found at and above N/P of 15:1

### 5.2 PgP/siMGMT polyplex characterization

The characteristics of the PgP/siRNA polyplex were next evaluated. The particle size, polydispersity index and zeta potential, or polyplex surface charge, are displayed in Table 2. The mean polyplex particle size found using the Zetasizer ZS was about 192 nm with a PDI of 0.19**.** The polydispersity index is expected for a micellar complex such as PgP/siRNA due to the

| (A) | PgP/siRNA | PgP/siRNA |
|---|---|---|
| N/P Ratio | **30:1** | **60:1** |
| Particle Size (nm) | 201.42 ± 4.17 | 192.2 ± 69.23 |
| PDI | 0.238 | 0.191 |
| Zeta Potential (mV) | 30.63 ± 1.60 | 47.5 ±6.72 |

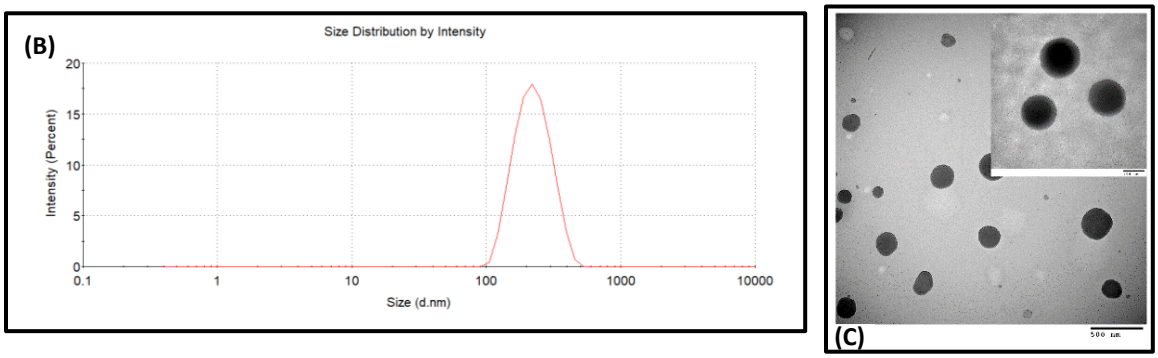


*Figure 6. Characterization of PgP/siMGMT.* (A) PgP/siMGMT polyplexes were characterized for particle size and zeta potential using a Zetasizer NS and N/P ratios of 30:1 and 60:1. (B) The distribution of particle size is graphed versus intensity, displaying the average particle size around 200 nm. (C)Transmission electron microscope (TEM) image of PgP-complexed siRNAs at a 30:1 N/P ratio. Gwak, S-J *et al.* (2016) *Acta Biomaterialia*, 35:98-108.

formulation methods. The zeta potential, a key indicator of the stability of colloidal dispersions, is about 48 mV, showing moderate stability (Fig. 6).

The net positive charge, from the positively charged PEI shell overcomes the siRNA's negative charge at this N/P of 60:1. Positively charged particles in the body have the tendency to interact with negatively charged proteins, which lead us to test PgP in heparin competition and serum protection assays. The polyplexes were imaged previously by Gwak et al., and displayed in in Figure 6. They were imaged with transmission electron microscope (TEM) at 30:1 are shown to create relatively uniformly sized and spherical polyplexes.[89]

### 5.3 PgP delivers siRNAs into glioblastoma cells *in vitro*

Once the ability of PgP to bind free siRNAs was confirmed, we examined the ability of PgP to deliver siRNAs into cells *in vitro.* T98G human glioblastoma cells were incubated with FI-siNT alone, or complexed with PEI, lipofectamine 2000, or PgP for 6 hours.

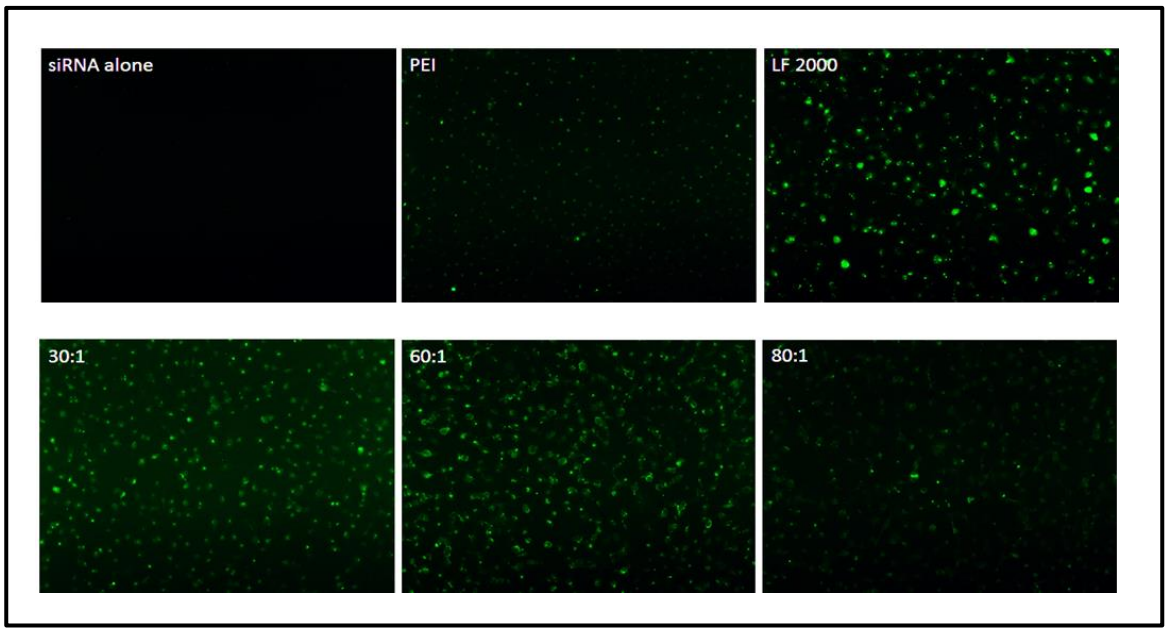


*Figure 7. PgP delivers siRNAs into GBM cell in vitro.* PgP at N/P ratios of 30:1, 60:1, and 80:1 mediates the uptake of green fluorescently labeled siRNA. Images taken my fluorescent microscopy 6 hours post-transfection.

Qualitatively, fluorescent microscopy revealed that the PgP/FI-siNT complex produced uptake of the siRNA in T98G cells, shown in figure 7. Both the intensity and amount of green fluorescence was taken into account when visually observing transfection. When delivered alone, siRNA does not appear to enter the cell, or remain intact. Visually, the optimal uptake was at N/P ratio of 60:1, but ratio 30:1 was similar. The N/P ratio of 80:1 appears to display a lower degree of uptake, but this is likely due to fluorescent signal quenching from the strong electrostatic interaction. Results were comparable to strong commercially available transfection agent Lipofectamine, and appeared to produce stronger signal than delivery with PEI.

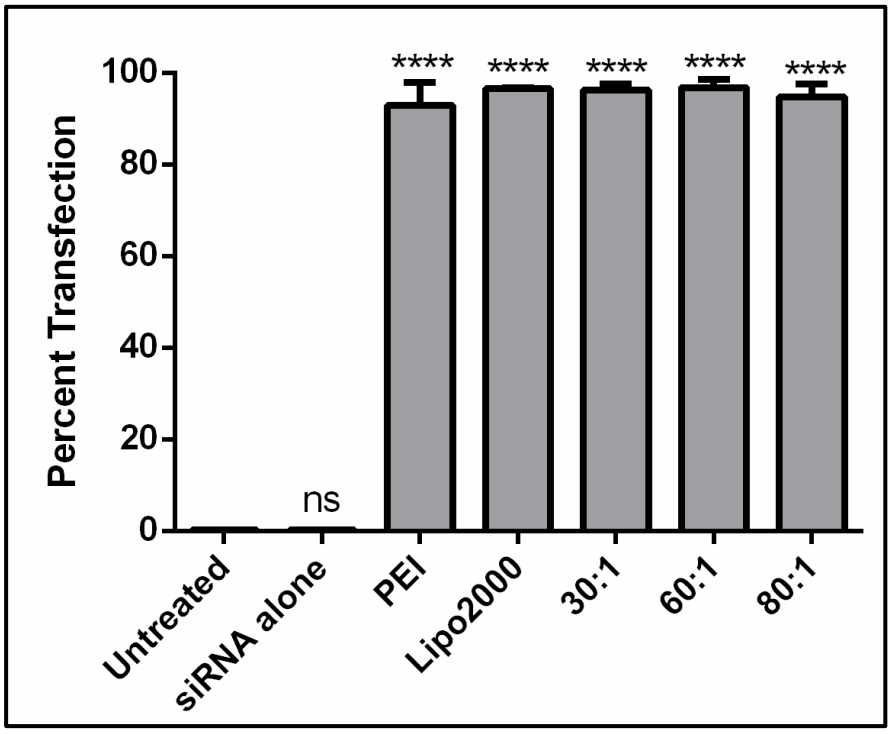


*Figure 8. PgP mediates uptake of siRNAs in human glioblastoma*. T98G cells with quantitative flow cytometry analysis of siRNA uptake in T98G cells 6 hours post-incubation with siRNA alone, or siRNA complexed with polyethyleneimine (PEI) at a 5:1 N/P ratio, Lipofectamine 2000 (Lipo2000), or PgP at a 30:1, 60:1, or 80:1 N/P ratios. Data are mean ± SEM of three independent experiments (N=3) where ****P<0.0001 or not significant (ns) compared to untreated cells (one-way ANOVA).

Flow cytometry was used to quantify the intracellular uptake of siRNA delivered by PgP 6 hours post-transfection. When quantified, no significant difference was seen between each ratio, or the positive transfection controls of PEI and LIPO2000. Over 90% transfection efficiency was observed in all PgP ratios, PEI and LIPO2000, confirming the efficacy of PgP as a nucleic acid delivery system. This data supports the theory that the discrepancy between qualitative and quantitative results is due to quenching from strong positive charge of PEI in both the PEI positive control and the PgP 80:1. The siRNA alone showed no significant uptake compared to the untreated control, suggesting that the cells had almost zero transfection.

**5.4 siRNA delivery displays minimal cytotoxicity in vitro**

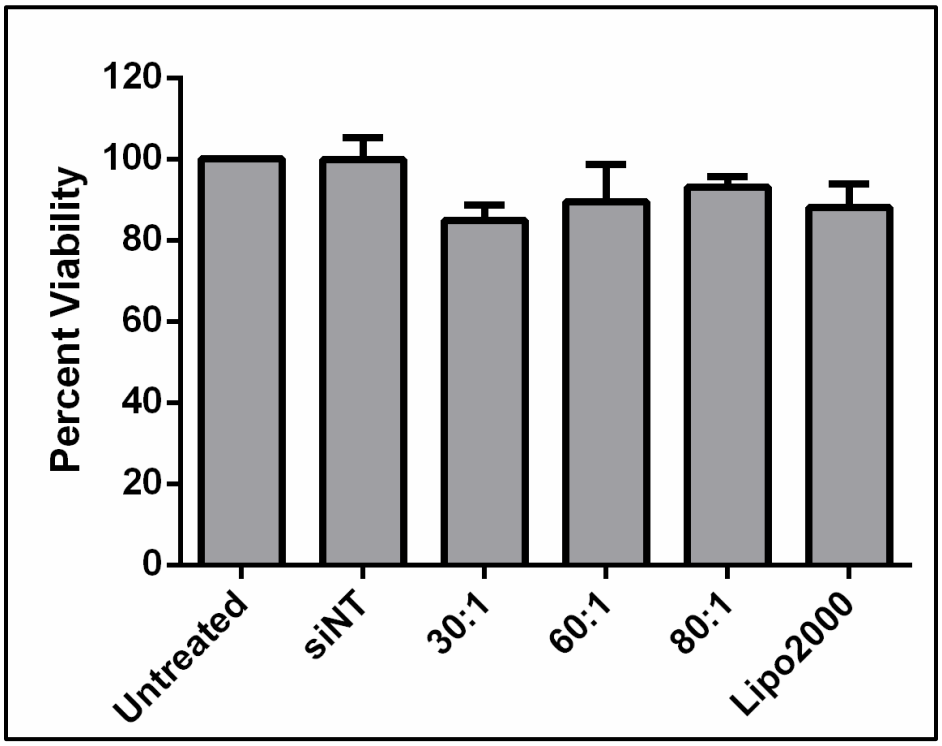


*Figure 9. PgP polyplexes display minimal cytotoxicity in T98G cells*. Quantitative analysis of T98G cell viability via MTT assay following 48-hour incubation with a non-targeting siRNA (siNT) alone or siNT complexed with Lipofectamine 2000 (Lipo2000) or PgP at a 30:1, 60:1, or 80:1 N/P ratio. Data are mean ± SEM of three independent experiments (N=3) performed in triplicate where the data is not significant compared to untreated cells (one-way ANOVA).

Cytotoxicity of the PgP polyplexes in T98G cells was determined by the performance of MTT assay after transfection. Cells were treated with siNT alone or complexed with LIPO2000, or PgP at N/P ratios of 30:1, 60:1 and 80:1. The results showed minimal cytotoxicity for all treatments in comparison to untreated cells (Fig. 9). The percent viabilities for cells treated with PgP polyplexes were 85%, 90%, and 93%, at N/P ratios of 30/1, 60/1, and 80/1, respectively, compared to 88% viability for cells treated the lipofectamine 2000/siNT. Overall these results demonstrate that PgP mediates efficient uptake of siRNAs into glioblastoma cells with minimal cytotoxicity, showing the potential utility of PgP as a vector for siRNA delivery.

### 5.5 Polyplexes enter the cell through endocytosis

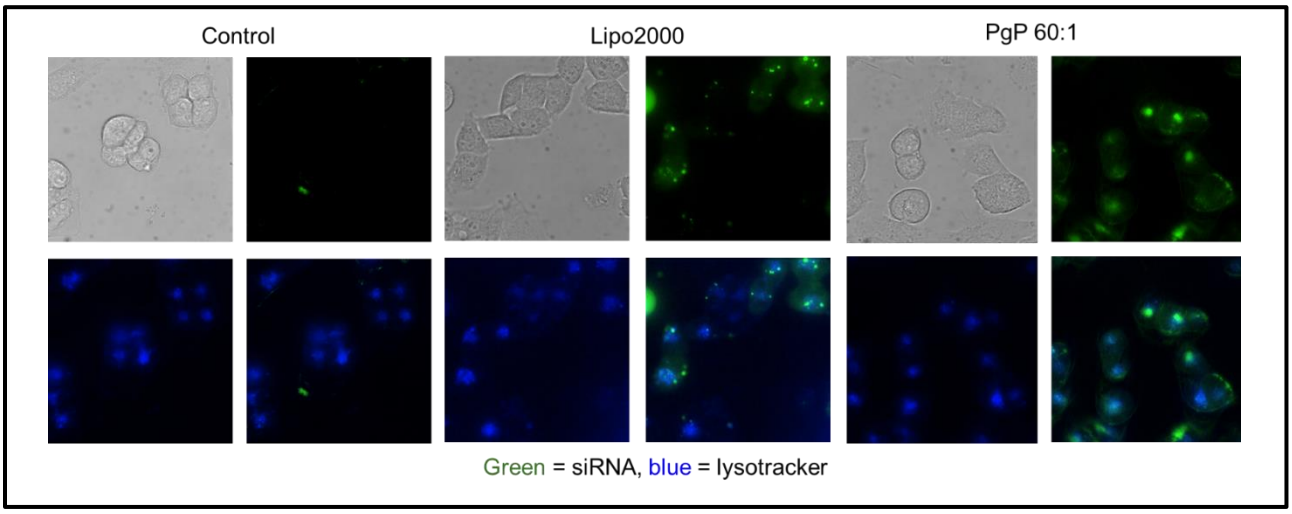


*Figure 10. PgP polyplexes enter the cell through endocytosis*. Endosomes were labeled with Lysotracker blue fluorescent label, and siRNA was labeled with green fluorescent FI-siNT. Colocalization of endosomes and siRNA suggested the cellular uptake of the polyplexes was occurring at the one hour timepoint.

Images of T98G cells were taken to visualize uptake after transfection and staining. The LysoTracker™ Blue stains the acidic organelles, indicating location of endosomes. Fluorescently labeled FI-siNT indicated location of the siRNA uptake within the cell. Fluorescent images of PgP/FI-siNT transfected cells showed colocalization of the endosomes and FI-siNT, indicating that the uptake of siRNA is mediated by endocytosis via endosomes. Images of the control, cells treated with siRNA alone, show that little green fluorescence remains after the incubation, but also that the clearly defined endosomes do not co-localize with the FI-siNT. Positive control LIPO2000 displays clear colocalization, comparable with that of PgP polyplexes. These results confirm the theorized method of cellular uptake of the polyplexes.

### 5.6 PgP mediates MGMT silencing

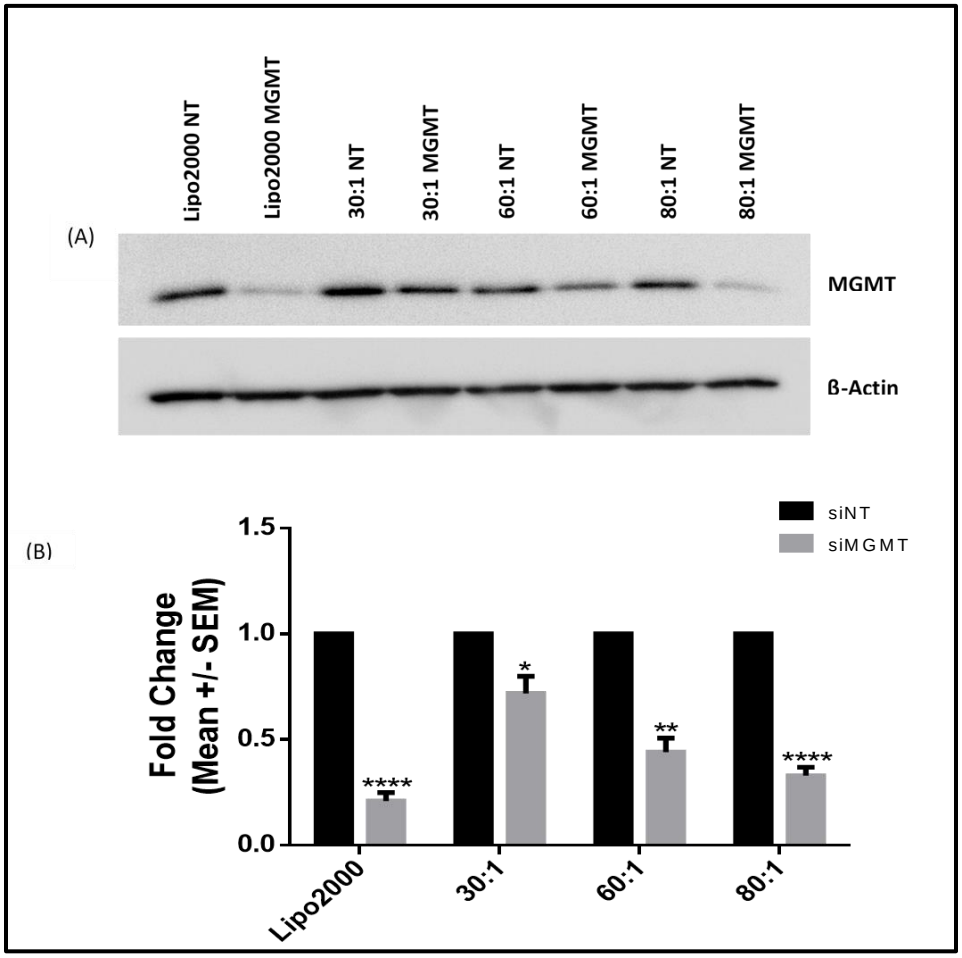


*Figure 11. PgP polyplexes mediate silencing of MGMT in T98G cells*. (A) Western blot analysis of MGMT protein levels or (B) Real-time PCR analysis of MGMT mRNA levels in T98G cells 48 hours post-treatment with siMGMT complexed with Lipofectamine 2000 (Lipo2000) or PgP at a 30:1, 60:1, or 80:1 N/P ratio, compared to cells treated with Lipo2000 or PgP complexed with non-targeting siRNA (siNT) at the same N/P ratio. β-Actin protein levels were monitored to ensure equal loading of samples. The MGMT mRNA levels were normalized to 18s endogenous mRNA levels. Data are mean ± SEM of three independent experiments performed in triplicate, where *P<0.05, **P<0.01, and ****P<0.0001 (t-test) compared to cells treated with siNT-complexed PgP or Lipo2000 at the same N/P ratio.

After the delivery efficiency and stability of the complex was determined, analysis of the silencing effect of siMGMT *in vitro* was evaluated. The silencing of MGMT was observed on the mRNA and protein levels. By performing a western blot, the knockdown of MGMT on the protein level can be visualized, as shown in Figure 11A. Positive protein control B-Actin is used to visualize that comparable protein is expressed in each sample. Comparing to non-targeting

controls, lighter bands are seen at N/P ratios of 30:1, 60:1 and 80:1, suggesting specificity of the gene silencing. Very significant reduction in expression is best visualized at N/P 80:1. At the mRNA level, knockdown was quantized using RT-PCR, displayed in Figure 11B. The expression was normalized to endogenously expressed 18s mRNA levels, and normalized to non-targeting controls to compare true percent expression in each sample. All N/P ratios display significant reduction in expression, and over 50% knockdown is seen at N/P 60:1 and 80:1. The N/P ratio of 60:1 was chosen to move forward with in studies, because of its significant ability to silence MGMT, while minimizing the amount of nucleic acid used. Minimization of the total siRNA amount is important in preventing possible toxicities *in vivo*.

### 5.7 PgP protects siRNA in physiological conditions

#### 5.7.1 Serum protection assays

To determine the ability of the PgP to protect siRNA from degradation in relevant physiological conditions, polyplexes were incubated with 10% or 50% serum (FBS) for 1 hour post-complexation. In images of polyplexes after electrophoresis, PgP shows to protect the siRNA after incubation in both 10% (Fig. 12A) and 50% serum (Fig. 12B), compared to when incubated in water. Protection is determined by the amount of siRNA that travels through the gel to the end compared to the negative control, siRNA alone, and positive controls PEI/siRNA and LIPO/siRNA, which are known to complex with and protect nucleic acids. After incubation in serum, the strong detergent SDS is used to dissociate the PgP from the siRNA, allowing remaining siRNA to run through the gel. When siRNA alone was incubated in serum conditions, little siRNA remains after the gel is run, compared with control siRNA incubated in water.

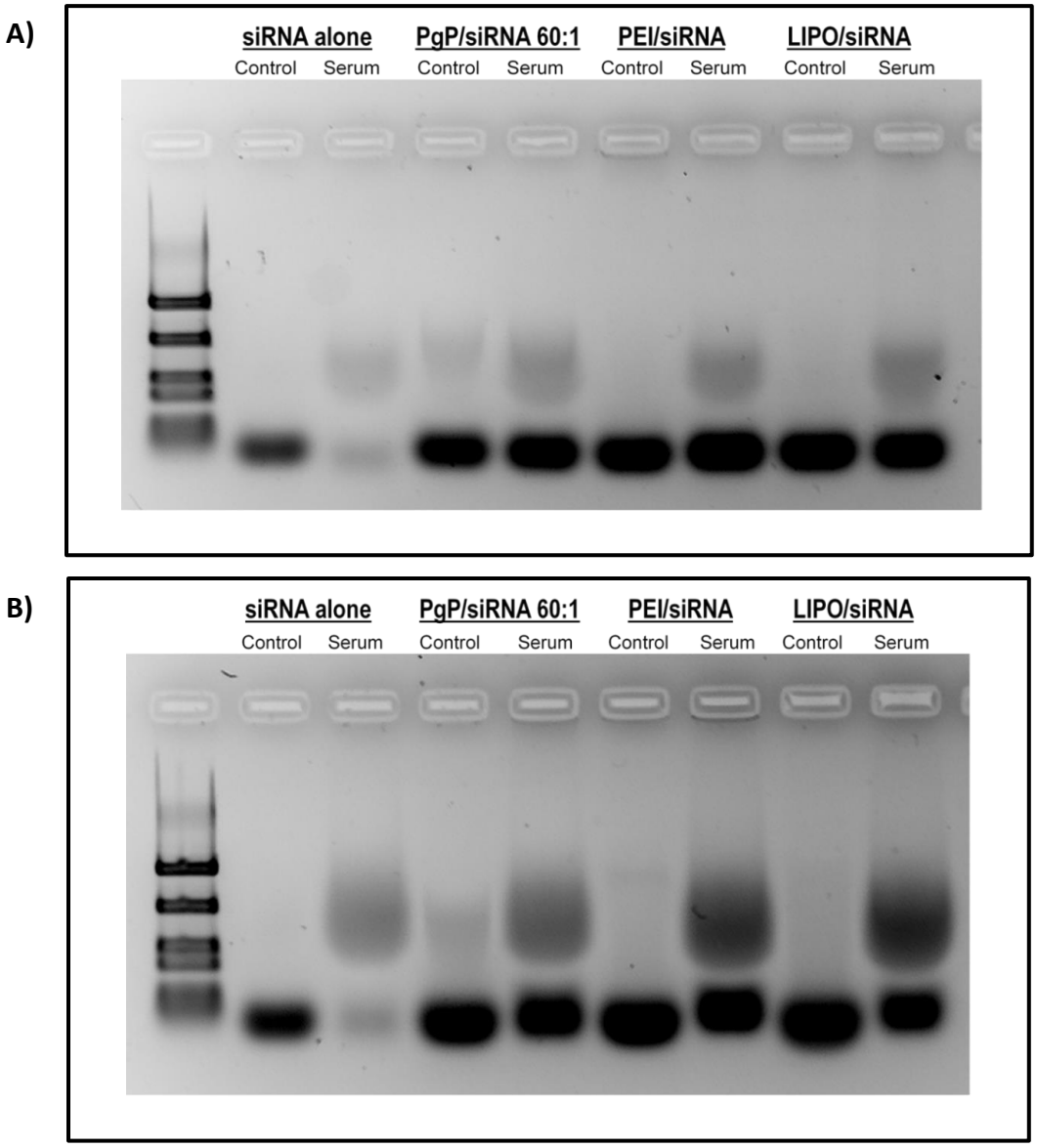


*Figure 12. Polyplexes protect siRNA from degradation in 10% and 50% serum conditions.* A) siRNA alone or complexed with PgP (N/P 60:1), PEI (N/P 5:1) and LIPO were incubated in A) 10% serum or B) 50% serum for 1 hour. Remaining siRNA at the bottom of the gel suggests PgP protects siRNA in 10% serum (A) and 50% serum (B).

Positive controls PEI/siRNA and LIPO/siRNA display maximal siRNA protection in serum and water, comparable to the siRNA protection seen with PgP. Streaking observed in the 10% and more heavily in the 50% gel is likely due to serum protein interactions or binding, where greater degree of binding is seen in the 50% serum than 10% serum conditions. Human blood conditions are comparable to 50% serum conditions, so although some protein binding was apparent, the

high degree of siRNA protection compared to controls confirms the ability of PgP to deliver siRNA *in vivo.*

### 5.7.2 RNase protection assay

PgP/siRNA 60:1 was next complexed and incubated for 1 hour in water or 0.01µg RNase A, a commercially available endoribonuclease that specifically degrades single-stranded RNA at C and U residues. When siRNA alone was incubated in RNase, no siRNA could be seen after the gel was run, indicating that the RNase will completely degrade ribonucleic acids. The PgP/siRNA complex shows no detectable degradation after RNAse incubation, compared with the complex incubated in water or positive controls PEI/siRNA and LIPO/siRNA.

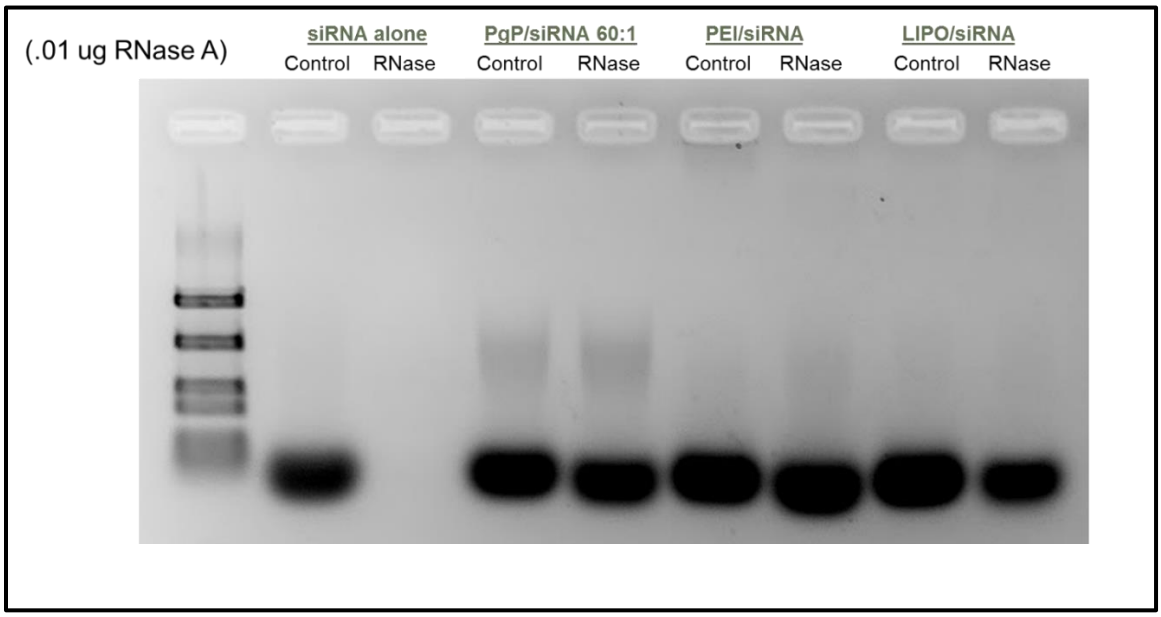


*Figure 13. Polyplexes protect siRNA from degradation due to ribonucleases*. siRNA alone or complexed with PgP (N/P 60:1), PEI (N/P 5:1) and LIPO were incubated in 0.01µg of RNase A. PgP shows to protect the siRNA from total degradation, as seen when siRNA alone is incubated in RNase A.

### 5.7.3 Heparin competition assay

PgP/siRNA 60:1 polyplexes were incubated with heparin at various weight ratios (WR, Heparin: siRNA) to assess competitive dissociation. The polyanion heparin is a negatively charged polysaccharide that can compete with nucleic acids for the interactions with polycations present, such as the PEI shell of PgP. After incubation, gel electrophoresis was run, and samples were compared to a control of siRNA alone, where the free siRNA ran through the gel completely. At a weight ratio of 5:1, dissociation of the PgP/siRNA polyplex begins, as some

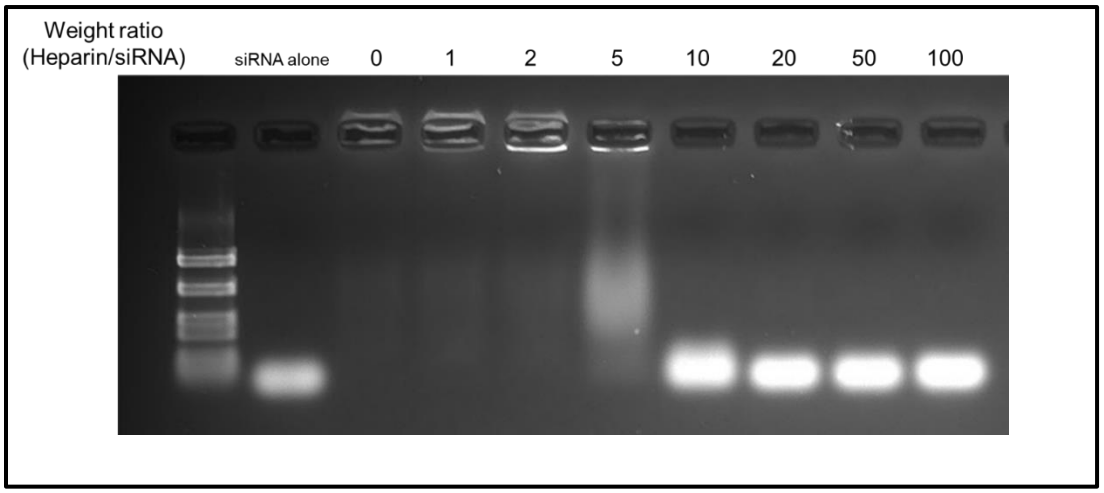


*Figure 14. Polyplexes remain stable in the presence of heparin up to a weight ratio (WR) of 10:1.* siRNA alone or complexed with PgP (N/P 60:1) was incubated with heparin at various weight ratios, ranging from 0 to 100. The polyplex shows stability up to the WR 5:1, where dissociation begins. Total dissociation is seen at WR of 10:1.

siRNA travels through the gel. At a WR of 10:1, the siRNA almost completely travels through the gel, suggesting that heparin competitively interacted with the complex and bound to the PgP, displacing siRNA. We can conclude that at some WR between 5:1 and 10:1, the polyplex does not completely dissociate, and at some WR between 2:1 and 5:1 and below, the polyplex is completely stable. These results demonstrate the stability of the polyplex in various physiological conditions, allowing us to predict the stability of the polyplexes *in vivo*.

### 5.8 Effect of MGMT knockdown on TMZ cytotoxicity

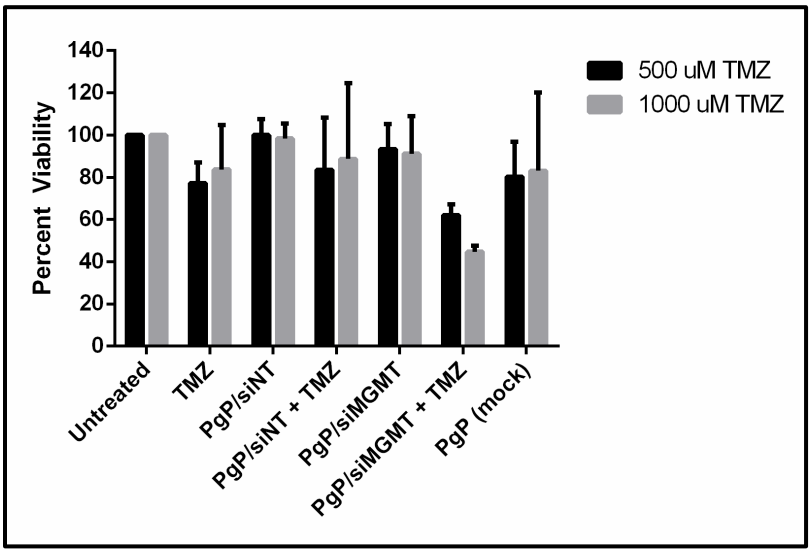


*Figure 15. Combination PgP/siMGMT and temozolomide treatment reduces viability of T98G cells*. Quantitative analysis of T98G cell viability via MTT assay 72 hours post-treatment with PgP-complexed siMGMT with or without concurrent temozolomide (TMZ) treatment of 500 or 1000 µM. Untreated cells and cells treated with PgP complexed with a non-targeting siRNA (siNT) were used as negative controls. Data are mean ± SEM of two independent experiments performed in triplicate.

The IC50 (half maximal inhibitory concentration), or 50% lethal dosage for TMZ in T98G cells was determined to be 1000µM TMZ. Once cells were treated with PgP/siMGMT or PgP/siNT, TMZ was added at 1000µM and 500um (half the IC50) and incubated for 72 hours. After 72 hours, an MTT assay was performed. Percent viability determined was normalized to untreated control. As displayed in Figure 15, a reduction in viability is apparent when PgP/siMGMT is used in combination with TMZ. After statistical analysis using one-way ANOVA, no significance was found between the PgP/siNT with TMZ group and the PgP/siMGMT with TMZ group. Therefore, a reduction in viability cannot yet be attributed to the silencing effect of siMGMT when treated in combination with TMZ. A reduction in cell viability is certainly apparent, but a larger sample size may be necessary for conclusive results.

### 5.9 Xenograft glioblastoma model in mouse brain was verified

#### 5.9.1 H&E staining

After injecting T98G cells into the mouse brains, the tumors were allowed to grow for 4 weeks. After 4 weeks, one mouse was sacrificed and the brain was harvested and preserved in 10% formalin for 24 hours and then 30% sucrose for 48 hours. Cryosectioning and Hematoxylin and Eosin (H&E) staining was performed to visualize the histological structure of the brain at the injection site. The slides prepared allowed us to see distinct tumor cells within the brain. As common with naturally occurring glioblastomas, the cells are diffuse and spread into the normal brain tissue, rather than forming a solid tumor mass. The cells can be identified in Figure 16, differentiated from normal tissue due to their fibroblastic morphology. At 2.5X, the injection site

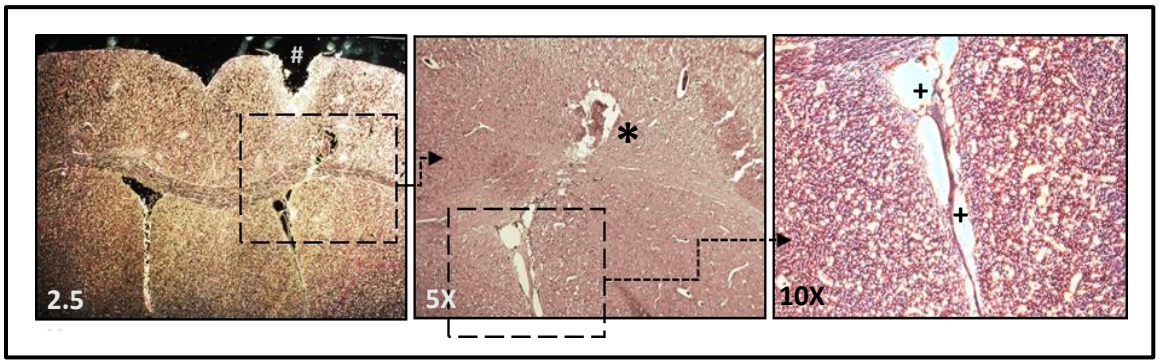


*Figure 16. Glioblastoma cells visualized within mouse brain tissue ex vivo.* At 2.5X magnification, the injection site can easily be seen, indicated by #. At 5x, a lesion is noted near the injection site, above the hippocampal region, indicated by *. At 10X, the fibroblastic glioblastoma cells can be seen spreading into the ventricle, indicated by +.

is easily visualized, where it has not healed fully. The sample shows that the right ventricle (side of injection) is significantly smaller than the left ventricle, suggesting that the GBM tissue has invaded the brain and is growing into the right ventricle. At 5X, the ventricle shows to have GBM cells within, and there is a lesion lateral and dorsal to the ventricle. At 10X, the cells can be more easily visualized, spreading throughout the ventricle.

### 5.9.2 Ex vivo imaging

After the polyplex injection and 72-hour incubation, the animals were sacrificed and brains removed. Brains were stored in RNAlater for 24 hours, and then placed into a mouse brain matrix for dissection. A slice was removed 1mm posterior and 1 mm anterior to the injection site (2mm total thickness). The slices were imaged with a dissection scope at 18X. The images showed the reduction in right ventricle size, compared to the left ventricle, for control, non-targeting and siMGMT groups, displayed in Figure 17.

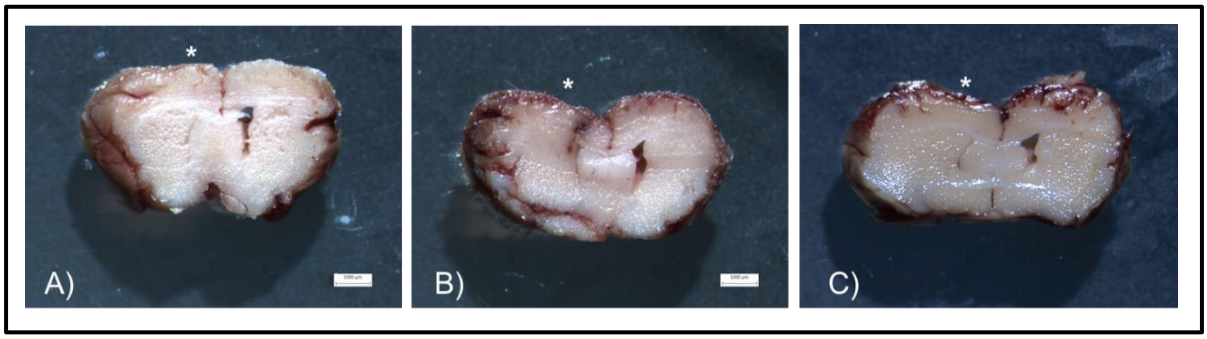


*Figure 17. GBM xenograft tumor model verified after sacrifice*. Reduction in ventricular space indicates tumor growth in the right hemisphere, where injection was performed. Asterik (*) indicates the approximate cellular and/or treatment injection location in (A) control group, (B) PgP/siNT group and (C) PgP/siMGMT treatment group.

### 5.10 DiR-loaded PgP/siNT remains in tumor for up to 10 days

IVIS imaging done at 1, 3, 6 and 24 hours, 48, 72 hours and then every 48 hours up to 10 days showed that the DiR-loaded polyplex remained in the brain tissue for at least 10 days. The minimum radiant efficiency was set to $5x10^6$ to allow for comparison across photos. The polyplex could be seen in the spleen with intensity after 24 hours and sporadically throughout imaging. The signal in the brain seems to remain consistent with each sampling. At 10 days after harvesting organs, the signal could be detected in the brain, but not in any other organs as seen in Figure 19. This suggests that the polyplex is accumulating in the brain tissue and remains for

up to 10 days without total clearance. The lack of signal in the rest of the organs suggests that there is no significant accumulation in peripheral organs. Clearance in the seen is expected, due to the nature of the positively charged polyplex, and the preference by the spleen to clear positively charged molecules.

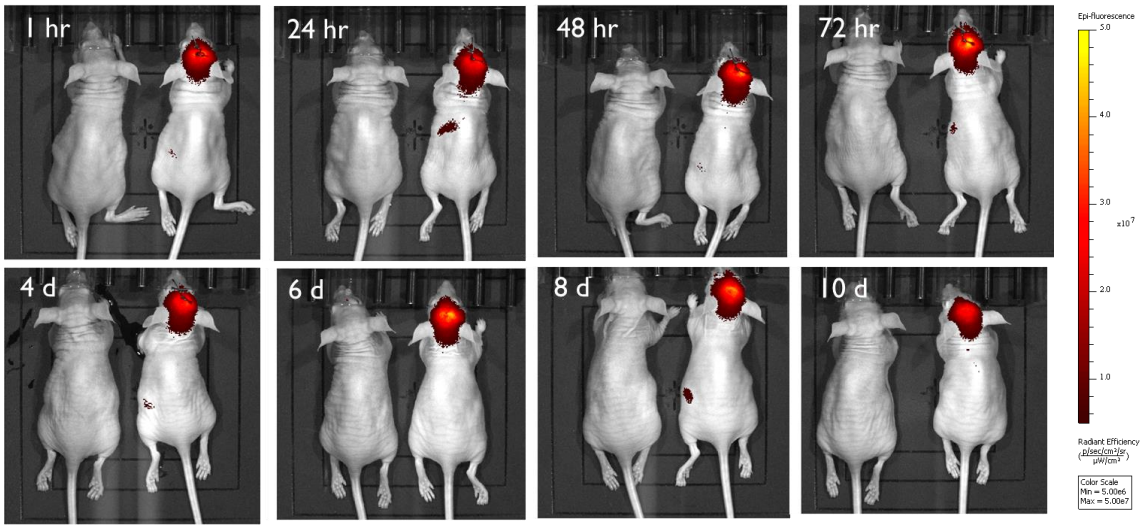


*Figure 18. Local delivery of DiR-loaded PgP/siNT into tumor site* (right mouse). Left mouse is control mouse with tumor but without DiR- PgP/siNT injection. A) 1 hour post injection, B) 24 hours post injection, C) 48 days post injection, D) 72 days hours post injection, E) 4 days post injection, F) 6 days post injection, G) 8 days post injection, H) 10 days post injection. Strong DiR signal is observed at each timepoint, with little reduction in strength over 72 hours.

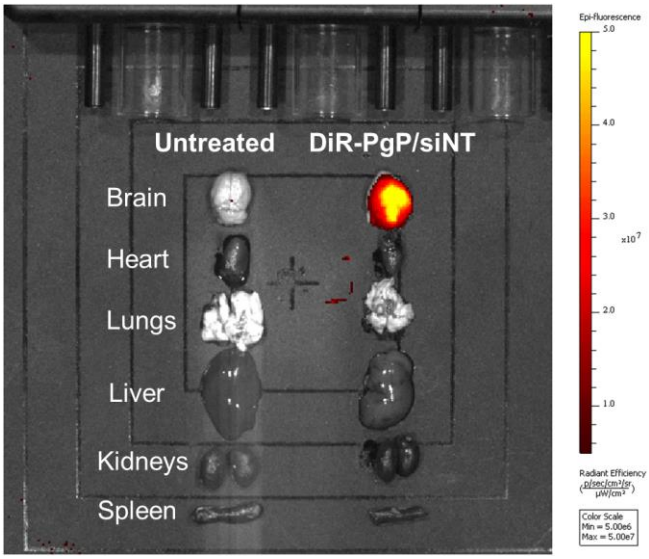


*Figure 19. DiR-loaded PgP/siNT remains in the brain tissue for at least 10 days*. Organs harvested from control mouse (right) versus DiR-PgP/siNT treated mouse (left). Organs from top to bottom: brain, heart, lungs, liver, kidneys, spleen. No polyplex accumulation is observed in organs after 10 days. Signal remains strong ($7.4 \times 10^7$ radiant efficiency) in the brain tissue 10 days post-injection.

**5.11 PgP/siMGMT polyplex mediates MGMT knockdown in vivo**

Once the polyplex biodistribution was evaluated in vivo, the therapeutic effect was studied. One month post-xenograpft, the mice were injected with either PgP/siNT, as a non-targeting control or PgP/siMGMT for therapy. Control mice were not injected with therapeutic, but were injected

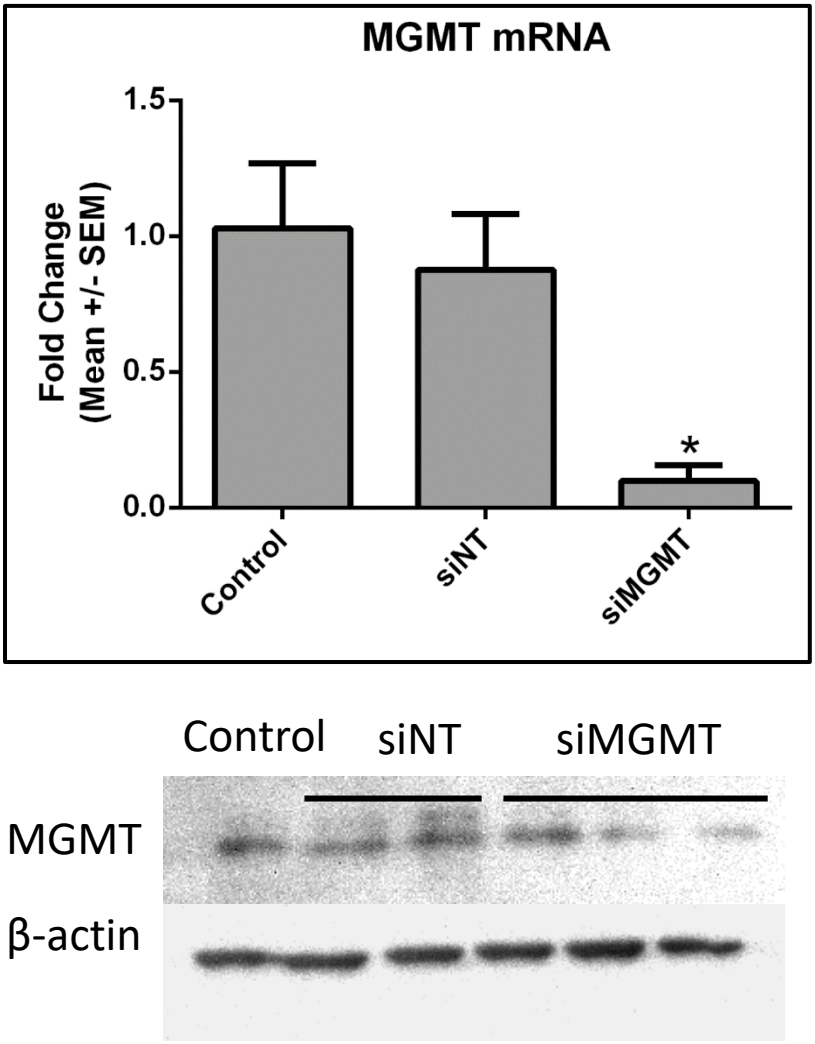


*Figure 20. PgP mediates knockdown of MGMT expression in vivo.* Expression of MGMT on the (A) mRNA and (B) protein levels of brain tumor tissue harvested 72-hours post-injection of PgP/siNT or PgP/siMGMT. Values are normalized to MGMT expression of control group. Data are mean ± SEM, where *P<0.05. β-actin as endogenously expressed protein control.

initially with the GBM cells. Brain tissue was harvested 72 hours post-injection. The silencing of MGMT mRNA was evaluated using RT-PCR, and results are displayed in Figure 20. The group of

mice treated with PgP/siMGMT shows significant reduction is MGMT expression compared to the control group, displayed in Figure 20A. There is no significant difference between the control group and the mice treated with PgP/siNT, suggesting that the non-targeting control did not knockdown MGMT. Western blot showed that the PgP/siMGMT had knockdown at the protein level compared to non-targeting and untreated controls, displayed in Figure 20B. These results are consistent with the silencing effect seen *in vitro,* and provide promise that PgP is an effective method of gene delivery *in vivo*. The safety of the therapy can be commented on, in that no deaths or adverse effects occurred within the 72 hours after injection.

# CHAPTER 6

# DISCUSSION

The overall goal of this project was to use our lab's novel delivery system, PgP, to effectively deliver siRNA *in vitro* and *in vivo,* to glioblastoma cells. Proving the efficacy and safety of siMGMT delivery would be relevant for the treatment of glioblastoma, in that it may allow for an increase in TMZ cytotoxicity. Increasing the toxicity would first allow for better treatment of the disease, eliminating more tumor cells from the body. It could further allow for lower dosages and therefore reduced toxic side effects, such as life-threatening myelosuppression.

After evaluating our results, there are a few highlights and a few limitations that should be addressed. First, the delivery system PgP has been shown to be very effective *in vitro* for delivery of siRNA into T98G cells. It provides for over 90% transfection and over 50% gene knockdown. However, *in vitro* conditions are very different from those of the human body, mainly in that we see cancer cells growing in a very controlled monolayer, compared to the unpredictable diffuse nature of gliomas in humans, where cancerous cells spread easily into normal regions of the brain. The H&E staining of brain sections gave us insight into the development of xenograft T98G tumors in nude mice. Although no visible tumor borders were clear, the individual GBM cells were apparent in the injected hemisphere, traveling easily through the ventricle. The *ex vivo* slicing of the brain tissue displayed clear asymmetry between the right and left hemispheres.

After DiR-PgP/siNT injections and imaging, the polyplex appears to remain stable in the brain tissue, and doesn't seem to accumulate in the peripheral organs. Though, there are limitations to the method of local delivery, in that it may not represent the accumulation of the polyplex in

the tumor if it were to be administered intravenously. Local injection was also used for the treatment administration, which is reasonable and potentially translatable to the clinic, but could cause high risk of local side effects such as infection. Minimizing the number of times that the skull is opened for surgery is preferred to reduce contact with pathogens, especially because treating infection in the brain is challenging.

After evaluating the gene silencing at the mRNA level *in vivo*, we can conclude that the delivery of siMGMT is feasible, but results had some inconsistencies. In order to determine the silencing effect with more accuracy, future studies should be done. Creating a tumor model using different cell lines may be more effective in creating solid tumors. Solid tumor tissue would allow for better removal of tissue and better analysis. It is likely that normal brain tissue was being analyzed within our tumor tissues, but in different amounts, causing variation in MGMT expression. Western blot displayed very light bands compared to β-actin control, suggesting that the MGMT levels are very low, even in control groups This may also give reason to the inconsistencies seen in the data after evaluating knockdown on the mRNA level.

The combinatorial studies done, where we attempted delivering siMGMT and TMZ either simultaneously or in sequence, did not provide conclusive results. The study may provide insight into the efficacy of TMZ in general. Studies done found that it was extremely difficult to produce cell death, even with high concentrations of TMZ applied directly to the cells. In comparison to 1000μM TMZ, the amount of CCNU to achieve IC50 on the T98G cells plated the same is only 50μM.  A more effective chemotherapeutic is needed to effectively kill GBM cells. The study may also be limited in the methods being used. MTT assay provide a measure of metabolic activity of the cells after treatment. A TUNEL assay may be attempted for future studies, where

the apoptotic activity of the cells is quantified. Because TMZ causes double stranded DNA breaks, this could be an appropriate method to more accurately determine the efficacy of the combination treatment. Increasing sample size further could provide for more reliable results.

Another outlook for this project would to be to effectively load an alkylating agent into the hydrophobic core of the PgP complex for more effective delivery of chemotherapeutics into glioblastoma cells. TMZ is nearly insoluble (5mg/ml) in water, so the hydrophobic core of PgP could potentially be an appropriate intermediate to delivery. Future work can be done with this to load the TMZ within the PgP and deliver the drug more effectively. Future work should include optimizing TMZ loading in PgP, as well as attempting to load other alkylating drugs such as lomustine (CCNU).

Further additions to the delivery system could include adding a targeting moiety and additional siRNA conjugates. A targeting moiety can be used to actively target the tumor tissue, in addition to the passive targeting technique. Possible treatments to be attempted in vivo could include: sequential delivery of PgP/siMGMT and then delivery of targeted TMZ-loaded PgP. Optimization of maximum MGMT knockdown *in vivo* should be determined, to administer the drug loaded PgP when it will be most effective. Additional siRNAs could be complexed with PgP, such as to interfere with oncogenic, tumor promoting genes, while providing an environment for TMZ to work optimally. Certain angiogenic genes that could be considered for knockdown include vascular endothelial growth factor (VEGF), epidermal growth factor receptor (EGFR), or platelet-derived growth factor (PDGF). EGFR and PDGF are overexpressed in primary and secondary GBM, respectively, therefore could have positive effects if silenced in different GBM patients. VEGF is a key angiogenic factor, allowing for vessel formation and tumor proliferation in many

cancer types, and is already being inhibited as a treatment for GBM (bevacizumab). The co-delivery of these siRNAs using the stable polymeric delivery system could further enhance treatment of GBM.

# CHAPTER 7

# CONCLUSION

In conclusion, it can be confirmed that PgP complexes with siRNAs and effectively mediates the delivery of siMGMT into T98G cells. It does so without significant cytotoxicity at N/P ratios of 30:1, 60:1 and 80:1. The PgP/siMGMT polyplex allows for significant reduction in expression on the mRNA and protein levels *in vitro*, with over 50 percent knockdown at using N/P ratios of 60:1 and 80:1. The N/P ratio of 60:1 was chosen as the ratio to move forward with in order to limit potential toxicity *in vivo,* by reducing total amount of reagent used, while still achieving over 50% gene silencing. Studies show that PgP protects siRNA from degradation in serum conditions and in the presence of ribonucleases, giving reason the believe that it will remain stable in the body.

*In vivo* results display the ability to grow T98G glioblastoma cells in nude mice, but the ability to form a solid tumor is not certain. Silencing of MGMT was found to be effective in mice on the mRNA and protein levels, however very little MGMT expression is apparent, causing variability in results. While significance is seen between the MGMT knockdown and control groups, the significance is only one star, where $P< 0.05$, reflecting these variabilities. The combination of PgP/siMGMT and TMZ shows decreased cell viability at 500µM and 1000µM, however no statistical significance was found between combination therapy of PgP/siMGMT + TMZ and combining PgP/siNT +TMZ. This may be due to in inability of TMZ to effectively kill glioblastoma cells, rather than the efficacy of the PgP/siMGMT polyplex.

Polymeric drug delivery shows great potential in the field of cancer treatment. Delivering drugs and genes using a multifunctional nanotherapeutic can help overcome the physical barrier of

the BBB, and combat chemotherapeutic resistance with gene therapy. PgP has great potential in becoming a new dual treatment for not only GBM, but many therapeutic areas. With further studies, we can hope to optimize the use of this carrier for the combinatorial delivery of siMGMT and TMZ, and bring longer lives to GBM patients.

# CHAPTER 8

# REFERENCES


1. Ostrom, Q. T. *et al.* CBTRUS statistical report: Primary brain and central nervous system tumors diagnosed in the United States in 2006 - 2010. *J. Neurooncol.* **15,** 788–796 (2013).

2. Alifieris, C. & Trafalis, D. T. Glioblastoma multiforme: Pathogenesis and treatment. *Pharmacol. Ther.* **152,** 63–82 (2015).

3. Louis, D. N. *et al.* The 2007 WHO classification of tumours of the central nervous system. *Acta Neuropathologica* **114,** 97–109 (2007).

4. Jhanwar-Uniyal, M., Labagnara, M., Friedman, M., Kwasnicki, A. & Murali, R. Glioblastoma: Molecular pathways, stem cells and therapeutic targets. *Cancers (Basel).* **7,** 538–555 (2015).

5. Holland, E. C. Glioblastoma multiforme: the terminator. *Proc. Natl. Acad. Sci. U. S. A.* **97,** 6242–6244 (2000).

6. Stupp, R., Hegi, M. E. & Mason, W. P. Effects of radiotherapy with concomitant and adjuvant temozolomide versus radiotherapy alone on survival in glioblastoma in a randomised phase III study: 5-year analysis of the EORTC-NCIC trial. *Lancet Oncol.* **10,** 459–466 (2009).

7. Hottinger, A. F., Stupp, R. & Homicsko, K. Standards of care and novel approaches in the management of glioblastoma multiforme. *Chin. J. Cancer* **33,** 32–39 (2014).

8. Bota, D. A., Desjardins, A., Quinn, J. A., Affronti, M. L. & Friedman, H. S. Interstitial chemotherapy with biodegradable BCNU (Gliadel?? ) wafers in the treatment of malignant gliomas. *Ther. Clin. Risk Manag.* **3,** 707–715 (2007).

9. Chowdhary, S. A., Ryken, T. & Newton, H. B. Survival outcomes and safety of carmustine wafers in the treatment of high-grade gliomas: a meta-analysis. *J. Neurooncol.* **122,** 367–382 (2015).

10. Cohen, M. H., Shen, Y. L., Keegan, P. & Pazdur, R. FDA drug approval summary: Bevacizumab (Avastin) as treatment of recurrent glioblastoma multiforme. *Oncologist* **14,** 1131–1138 (2009).

11. Van Tellingen, O. *et al.* Overcoming the blood-brain tumor barrier for effective glioblastoma treatment. *Drug Resist. Updat.* **19,** 1–12 (2015).

12. Rong, Y. *et al.* Early growth response gene-1 regulates hypoxia-induced expression of tissue factor in glioblastoma multiforme through hypoxia-inducible factor-1-independent mechanisms. *Cancer Res.* **66,** 7067–7074 (2006).

13. Kleihues, P. & Ohgaki, H. Primary and secondary glioblastomas: from concept to clinical diagnosis. *Neuro. Oncol.* **1,** 44–51 (1999).

14. Wrensch, M., Minn, Y., Chew, T., Bondy, M. & Berger, M. S. Epidemiology of primary brain tumors: current concepts and review of the literature. *Neuro Oncol* **4,** 278–299 (2002).

15. Burch, J. D. *et al.* An exploratory case-control study of brain tumors in adults. *J. Natl. Cancer Inst.* **78,** 601–609 (1987).

16. Zahm, S. H. & Ward, M. H. Pesticides and childhood cancer. in *Environmental Health Perspectives* **106,** 893–908 (1998).

17. Vogelstein, B. & Kinzler, K. W. The multistep nature of cancer. *Trends in Genetics* **9,** 138–141 (1993).

18. Verhaak, R., Hoadley, K., Purdon, E. & Getz, G. An integrated genomic analysis identifies clinically relevant subtypes of glioblastoma characterized by abnormalities in PDGFRA, IDH1, EGFR and NF1. *Cancer Cell* **19,** 38–

46 (2010).

19. Hay, N. & Sonenberg, N. Upstream and downstream of mTOR. *Genes and Development* **18,** 1926–1945 (2004).

20. Louis, D. N. Molecular Pathology of Malignant Gliomas. *Annu. Rev. Pathol. Mech. Dis.* **1,** 97–117 (2006).

21. Gomez-Manzano, C. *et al.* Adenovirus-mediated transfer of the p53 gene produces rapid and generalized death of human glioma cells via apoptosis. *Cancer Res.* **56,** 694–699 (1996).

22. Yoshino, A. *et al.* Effect of IFN-beta on human glioma cell lines with temozolomide resistance. *Int. J. Oncol.* **151,** 414–420 (2009).

23. Stupp, R. *et al.* Radiotherapy plus Concomitant\nand Adjuvant Temozolomide for Glioblastoma. *N. Engl. J. Med.* 987–96 (2005). doi:10.1056/NEJMoa043330

24. Mrugala, M. M. & Chamberlain, M. C. Mechanisms of Disease: temozolomide and glioblastoma—look to the future. *Nat. Clin. Pract. Oncol.* **5,** 476–486 (2008).

25. Hegi, M. E. *et al.* MGMT gene silencing and benefit from temozolomide in glioblastoma. *N. Engl. J. Med.* **352,** 997–1003 (2005).

26. Westphal, M. *et al.* A phase 3 trial of local chemotherapy with biodegradable carmustine (BCNU) wafers (Gliadel wafers) in patients with primary malignant glioma. *Neuro. Oncol.* **5,** 79–88 (2003).

27. Wait, S. D., Prabhu, R. S., Burri, S. H., Atkins, T. G. & Asher, A. L. Polymeric drug delivery for the treatment of glioblastoma. *Neuro. Oncol.* **17,** ii9-ii23 (2015).

28. Zhou, J. *et al.* Highly penetrative , drug-loaded nanocarriers improve treatment of glioblastoma. (2013). doi:10.1073/pnas.1304504110

29. Maxwell, M. *et al.* Expression of angiogenic growth factor genes in primary human astrocytomas may contribute to their growth and progression. *Cancer Res.* **51,** 1345–51 (1991).

30. Kreisl, T. N. *et al.* Phase II trial of single-agent bevacizumab followed by bevacizumab plus irinotecan at tumor progression in recurrent glioblastoma. *J. Clin. Oncol.* **27,** 740–745 (2009).

31. Banks, W. A. Characteristics of compounds that cross the blood-brain barrier. *BMC Neurol.* **9,** S3 (2009).

32. Horio, M., Gottesman, M. M. & Pastan, I. ATP-dependent transport of vinblastine in vesicles from human multidrug-resistant cells. *Proc Natl Acad Sci U S A* **85,** 3580–4 (1988).

33. Schinkel, A. H., Wagenaar, E., Mol, C. A. A. M. & Van Deemter, L. P-glycoprotein in the blood-brain barrier of mice influences the brain penetration and pharmacological activity of many drugs. *J. Clin. Invest.* **97,** 2517–2524 (1996).

34. Choo, E. F. *et al.* Differential in vivo sensitivity to inhibition of P-glycoprotein located in lymphocytes, testes, and the blood-brain barrier. *J. Pharmacol. Exp. Ther.* **317,** 1012–1018 (2006).

35. Peer, D. *et al.* Nanocarriers as an emerging platform for cancer therapy. *Nat. Nanotechnol.* **2,** 751–760 (2007).

36. Kamaly, N., Xiao, Z., Valencia, P. M., Radovic-Moreno, A. F. & Farokhzad, O. C. Targeted polymeric therapeutic nanoparticles: design, development and clinical translation. *Chem Soc Rev* **41,** 2971–3010 (2012).

37. Kim, S. S., Harford, J. B., Pirollo, K. F. & Chang, E. H. Effective treatment of glioblastoma requires crossing the blood-brain barrier and targeting tumors including cancer stem cells: The promise of nanomedicine. *Biochemical and Biophysical Research Communications* **468,** 485–489 (2015).

38. Hardee, M. E. & Zagzag, D. Mechanisms of glioma-associated neovascularization. *American Journal of Pathology* **181,** 1126–1141 (2012).

39. S??h??dic, D., Cikankowitz, A., Hindr??, F., Davodeau, F. & Garcion, E. Nanomedicine to overcome radioresistance in glioblastoma stem-like cells and surviving clones. *Trends Pharmacol. Sci.* **36,** 236–252 (2015).

40. Hegi, M. & Diserens, A. MGMT gene silencing and benefit from temozolomide in glioblastoma. *N. Engl. J. Med.* **352,** 997–1003 (2005).

41. Zhang, J., Stevens, M. F. G. & Bradshaw, T. D. Temozolomide: Mechanisms of Action, Repair and Resistance. *Curr. Mol. Pharmacol.* **5,** 102–114 (2012).

42. Tolcher, A. W. *et al.* Marked inactivation of O6-alkylguanine-DNA alkyltransferase activity with protracted temozolomide schedules. *Br. J. Cancer* **88,** 1004–1011 (2003).

43. Munoz, J. L. *et al.* Temozolomide Induces the Production of Epidermal Growth Factor to Regulate MDR1 Expression in Glioblastoma Cells. *Mol. Cancer Ther.* **13,** 2399–2411 (2014).

44. Donson, A. M., Addo-Yobo, S. O., Handler, M. H. M., Gore, L. M. & Foreman, N. K. MGMT Promoter Methylation Correlates With Survival Benefit and Sensitivity to Temozolomide in Pediatric Glioblastoma. *J. Clin. Oncol.* **14,** 1526–1531 (1996).

45. Warren, K. E. *et al.* A Phase II Study of O6-Benzylguanine and Temozolomide in Pediatric Patients with Recurrent or Progressive High Grade Gliomas and Brainstem Gliomas: A Pediatric Brain Tumor Consortium. *J Neurooncol* **106,** 643–649 (2012).

46. Kato, T. *et al.* Efficient delivery of liposome-mediated MGMT-siRNA reinforces the cytotoxity of temozolomide in GBM-initiating cells. *Gene Ther.* **17,** 1363–1371 (2010).

47. de Faria, G. P. & de Oliveria, J. A. Differences in the Expression Pattern of P-Glycoprotein and MRP1 in Low-Grade and High-Grade Gliomas. *Cancer Invest.* **26,** 883–889 (2008).

48. Beier, D., Schulz, J. B. & Beier, C. P. Chemoresistance of glioblastoma cancer stem cells - much more complex than expected. *Mol. Cancer* **10,** 128 (2011).

49. Van Den Bent, M. J. *et al.* Randomized phase II trial of erlotinib versus temozolomide or carmustine in recurrent glioblastoma: EORTC brain tumor group study 26034. *J. Clin. Oncol.* **27,** 1268–1274 (2009).

50. Hegi, M. E. *et al.* Pathway Analysis of Glioblastoma Tissue after Preoperative Treatment with the EGFR Tyrosine Kinase Inhibitor Gefitinib--A Phase II Trial. *Mol. Cancer Ther.* **10,** 1102–1112 (2011).

51. Neyns, B. *et al.* Stratified phase II trial of cetuximab in patients with recurrent high-grade glioma. *Ann. Oncol.* **20,** 1596–1603 (2009).

52. Wang, K., Park, J. O. & Zhang, M. Treatment of glioblastoma multiforme using combination of siRNA targeting EGFR and β-catenin. *J. Gene Med.* **15,** 42–50 (2013).

53. Den, R. B. *et al.* A phase i study of the combination of sorafenib with temozolomide and radiation therapy for the treatment of primary and recurrent high-grade gliomas. *Int. J. Radiat. Oncol. Biol. Phys.* **85,** 321–328 (2013).

54. Lee, E. Q. *et al.* Phase I/II study of sorafenib in combination with temsirolimus for recurrent glioblastoma or gliosarcoma: North American Brain Tumor Consortium study 05-02. *Neuro. Oncol.* **14,** 1511–1518 (2012).

55. Reardon, D. A. *et al.* Effect of CYP3A-inducing anti-epileptics on sorafenib exposure: Results of a phase II study of sorafenib plus daily temozolomide in adults with recurrent glioblastoma. *J. Neurooncol.* **101,** 57–66 (2011).

56. Sonabend, A. M., Ulasov, I. V & Lesniak, M. S. Gene therapy trials for the treatment of high-grade gliomas. *Gene Ther. Mol. Biol.* **11,** 79–92 (2007).

57. Oldfield, E. H. *et al.* Gene therapy for the treatment of brain tumors using intra-tumoral transduction with

the thymidine kinase gene and intravenous ganciclovir. *Hum. Gene Ther.* **4,** 39–69 (1993).

58. Braun, E. Neurotropism of herpes simplex virus type 1 in brain organ cultures. *J. Gen. Virol.* **87,** 2827–2837 (2006).

59. Peltékian, E., Garcia, L. & Danos, O. Neurotropism and Retrograde Axonal Transport of a Canine Adenoviral Vector: A Tool for Targeting Key Structures Undergoing Neurodegenerative Processes. *Mol. Ther.* **5,** 25–32 (2002).

60. Kim, S. H., Xiao, S., Shive, H., Collins, P. L. & Samal, S. K. Replication, neurotropism, and pathogenicity of avian paramyxovirus serotypes 1-9 in chickens and ducks. *PLoS One* **7,** (2012).

61. Okura, H., Smith, C. A. & Rutka, J. T. Gene therapy for malignant glioma. *Mol. Cell. Ther.* **2,** 21 (2014).

62. Rainov, N. A phase III clinical evaluation of herpes simplex virus type 1 thymidine kinase and ganciclovir gene therapy as an adjuvant to surgical resection and radiation in adults with previously untreated glioblastoma multiforme. *Hum. Gene Ther.* **11,** 2389–401 (2000).

63. Aguilar, L. K. *et al.* Phase II multicenter study of gene mediated cytotoxic immunotherapy as adjuvant to surgical resection for newly diagnosed malignant glioma. *J Clin Oncol (Meeting Abstr.* **33,** 2010 (2015).

64. Kalkanis, S. *et al.* Intravenous Administration of Toca 511 in Patients With Recurrent Glioblastoma. *Neuro. Oncol.* **16,** v15–v15 (2014).

65. Zhang, J. & Saltzman, M. Engineering biodegradable nanoparticles for drug and gene delivery. *Chem. Eng. Prog.* **109,** 25–30 (2013).

66. Waite, C. L. & Roth, C. M. PAMAM-RGD Conjugates Enhance siRNA Delivery Through a Multicellular Spheroid Model of Malignant Glioma. *Bioconjug Chem* **20,** 1908–1916 (2011).

67. Wang, S. *et al.* The role of autophagy in the neurotoxicity of cationic PAMAM dendrimers. *Biomaterials* **35,** 7588–7597 (2014).

68. Mangraviti, A. *et al.* Polymeric nanoparticles for nonviral gene therapy extend brain tumor survival in vivo. *ACS Nano* **9,** 1236–1249 (2015).

69. Guerrero-Cázares, H. *et al.* Biodegradable Polymeric Nanoparticles Show High Efficacy and Specificity at DNA Delivery to Human Glioblastoma *in Vitro* and *in Vivo*. *ACS Nano* **8,** 5141–5153 (2014).

70. Zhan, C. *et al.* Cyclic RGD-polyethylene glycol-polyethylenimine for intracranial glioblastoma-targeted gene delivery. *Chem. - An Asian J.* **7,** 91–96 (2012).

71. de Lima, M. C. *et al.* Gene delivery mediated by cationic liposomes: from biophysical aspects to enhancement of transfection. *Mol Membr Biol* **16,** 103–109 (1999).

72. Balazs, D. A. & Godbey, W. Liposomes for Use in Gene Delivery. *J. Drug Deliv.* **2011,** 1–12 (2011).

73. Lin, Q. *et al.* Brain tumor-targeted delivery and therapy by focused ultrasound introduced doxorubicin-loaded cationic liposomes. *Cancer Chemother. Pharmacol.* **77,** 269–280 (2016).

74. Calcagno, C., Lobatto, M. E., Robson, P. M. & Millon, A. Encapsulation of temozolomide in a tumor-targeting nanocomplex enhances anti-cancer efficacy and reduces toxicity in a mouse model of glioblastoma. *Cancer Lett.* **28,** 1304–1314 (2015).

75. Qu, J. *et al.* Nanostructured lipid carriers, solid lipid nanoparticles, and polymeric nanoparticles: which kind of drug delivery system is better for glioblastoma chemotherapy? *Drug Deliv.* **23,** 3408–3416 (2016).

76. Chen, Z., Lai, X., Song, S., Zhu, X. & Zhu, J. Nanostructured lipid carriers based temozolomide and gene co-encapsulated nanomedicine for gliomatosis cerebri combination therapy. *Drug Deliv.* **23,** 1369–73 (2016).

77. Guo, W., Chen, W., Yu, W., Huang, W. & Deng, W. Small interfering RNA-based molecular therapy of cancers.

*Chin. J. Cancer* **32,** 488–493 (2013).

78. Mansoori, B., Shotorbani, S. S. & Baradaran, B. RNA interference and its role in cancer therapy. *Adv. Pharm. Bull.* **4,** 313–321 (2014).

79. Yoo, B., Ifediba, M. A., Ghosh, S., Medarova, Z. & Moore, A. Combination treatment with theranostic nanoparticles for glioblastoma sensitization to TMZ. *Mol. Imaging Biol.* **16,** 680–689 (2014).

80. Kanasty, R., Dorkin, J. R., Vegas, A. & Anderson, D. Delivery materials for siRNA therapeutics. *Nat Mater* **12,** 967–977 (2013).

81. Jones, S. K. & Merkel, O. M. Tackling breast cancer chemoresistance with nano-formulated siRNA. *Gene Ther.* **23,** 821–828 (2016).

82. Fenstermaker, R. A. *et al.* Clinical study of a survivin long peptide vaccine (SurVaxM) in patients with recurrent malignant glioma. *Cancer Immunol. Immunother.* **65,** 1339–1352 (2016).

83. Aucouturier, J., Dupuis, L., Deville, S., Ascarateil, S. & Ganne, V. Montanide ISA 720 and 51: a new generation of water in oil emulsions as adjuvants for human vaccines. *Expert Rev. Vaccines* **1,** 111–118 (2002).

84. Liu, Y., Miao, C., Wang, Z., He, X. & Shen, W. Survivin small interfering RNA suppresses glioblastoma growth by inducing cellular apoptosis. *Neural Regen. Res.* **7,** 924–931 (2012).

85. Portnow, J. *et al.* Neural Stem Cell–Based Anticancer Gene Therapy: A First-in-Human Study in Recurrent High-Grade Glioma Patients. *Clin. Cancer Res.* (2016). doi:10.1158/1078-0432.CCR-16-1518

86. Kim, S.-S., Rait, A., Kim, E., Pirollo, K. F. & Chang, E. H. A Tumor-targeting p53 Nanodelivery System Limits Chemoresistance to Temozolomide Prolonging Survival in a Mouse Model of Glioblastoma Multiforme Sang-Soo. *J. Nanomedicine* **11,** 301–311 (2015).

87. Quinn, J. A. *et al.* Phase II Trial of Temozolomide Plus O6-Benzylguanine in Adults with Recurrent, Temozolomide-Resistant Malignant Glioma. *J. Clin. Oncol.* **27,** 1262–1267 (2009).

88. Pirollo, K. F. *et al.* Safety and Efficacy in Advanced Solid Tumors of a Targeted Nanocomplex Carrying the p53 Gene Used in Combination with Docetaxel: A Phase 1b Study. *Mol. Ther.* **24,** 1697–1706 (2017).

89. Gwak, S.-J. *et al.* Cationic, amphiphilic copolymer micelles as nucleic acid carriers for enhanced transfection in rat spinal cord. *Acta Biomater.* **18,** 1067–1073 (2015).